This paper is available on line at http://www.mcponline.org

Quantitative Proteomics of the *Neisseria Gonorrhoeae* Cell Envelope and Membrane Vesicles for the Discovery of Potential Therapeutic Targets*[S]

Ryszard A. Zielke‡, Igor H. Wierzbicki‡, Jacob V. Weber‡, Philip R. Gafken§, and Aleksandra E. Sikora‡¶

Neisseria gonorrhoeae **(GC) is a human-specific pathogen, and the agent of a sexually transmitted disease, gonorrhea. There is a critical need for new approaches to study and treat GC infections because of the growing threat of multidrug-resistant isolates and the lack of a vaccine. Despite the implied role of the GC cell envelope and membrane vesicles in colonization and infection of human tissues and cell lines, comprehensive studies have not been undertaken to elucidate their constituents. Accordingly, in pursuit of novel molecular therapeutic targets, we have applied isobaric tagging for absolute quantification coupled with liquid chromatography and mass spectrometry for proteome quantitative analyses. Mining the proteome of cell envelopes and native membrane vesicles revealed 533 and 168 common proteins, respectively, in analyzed GC strains FA1090, F62, MS11, and 1291. A total of 22 differentially abundant proteins were discovered including previously unknown proteins. Among those proteins that displayed similar abundance in four GC strains, 34 were found in both cell envelopes and membrane vesicles fractions. Focusing on one of them, a homolog of an outer membrane protein LptD, we demonstrated that its depletion caused loss of GC viability. In addition, we selected for initial characterization six predicted outer membrane proteins with unknown function, which were identified as ubiquitous in the cell envelopes derived from examined GC isolates. These studies entitled a construction of deletion mutants and analyses of their resistance to different chemical probes. Loss of NGO1985, in particular, resulted in dramatically decreased GC viability upon treatment with detergents, polymyxin B, and chloramphenicol, suggesting that this protein functions in the maintenance of the cell envelope permeability barrier. Together, these findings underscore the concept that the cell envelope and membrane vesicles contain crucial, yet under-explored determinants of GC physiology, which may represent promising targets for designing new therapeutic interventions.** ***Molecular & Cellular Proteomics 13: 10.1074/mcp.M113.029538, 1299–1317, 2014.***

Neisseria gonorrhoeae (GC)[1] is an obligate human pathogen and the etiological agent of gonorrhea, a sexually transmitted disease. GC infection remains a significant health and economic burden worldwide (1). It is also the second most commonly reported infectious disease in the United States (2). Gonorrhea ranges from clinically asymptomatic to local genital infections to disseminated bloodstream infections. Asymptomatic infections often have devastating consequences on women's health including pelvic inflammatory disease, ectopic pregnancy, and infertility (3). Additionally, GC infections facilitate transmission and acquisition of HIV (4). For all of these reasons it is critical to provide effective treatments against gonorrhea. Currently, a dual therapy with cephalosporin and either azithromycin or doxycycline is recommended (5). However, over the past several years treatment failures associated with GC strains displaying decreased susceptibility to extended spectrum cephalosporins have been reported from various parts of the world (6–9). This is especially concerning because no other antibiotics are clinically useful in these cases, and because no appropriate vaccine exists (10). The escalating problem of the spread of antimicrobial resistance in GC, and the importance of the develop-

From the ‡Department of Pharmaceutical Sciences, College of Pharmacy, Oregon State University, Corvallis, Oregon 97331; §Proteomics Facility, Fred Hutchinson Cancer Research Center, Seattle, Washington 98109-1024

Received March 26, 2013, and in revised form, February 28, 2014
Published, MCP Papers in Press, March 8, 2014, DOI 10.1074/mcp.M113.029538

Author contributions: R.A.Z. and A.E.S. designed research; R.A.Z., I.H.W., J.V.W., P.R.G., and A.E.S. performed research; R.A.Z., P.R.G., and A.E.S. analyzed data; R.A.Z., P.R.G., and A.E.S. wrote the paper.

[1] The abbreviations used are: GC, *Neisseria gonorrhoeae*; ACN, acetonitrile; CE, cell envelopes; CFU, colony-forming units; COG, Clusters of Orthologous Groups; GCB, GC agar plates; GCBL, GC broth liquid medium; IPTG, isopropyl-β-D-galactopyranoside; iTRAQ, isotope tagging for relative and absolute quantification; LPS, lipopolysaccharide; MVs, membrane vesicles; 2D-LC, two-dimensional liquid chromatography; SCX, strong cation exchange; TFA, trifluoroacetic acid.

ment of new approaches to study, treat, and prevent GC infection, have been recognized by the World Health Organization and by the Centers for Disease Control and Prevention (11, 12).

We propose that largely unexplored proteins localized to bacterial cell envelope and naturally released membrane vesicles are particularly promising as potential novel molecular targets for therapeutic interventions against gonorrhea. The small fraction of known components of the GC cell envelope (outer membrane, periplasm, cytoplasmic membrane) plays a fundamental role in establishing infection by enabling the microbes to adhere to and invade host cells, facilitating nutrient acquisition, host tissue destruction, and suppression of immune responses (3, 13–15). Further, GC, like many other Gram-negative bacteria, produces membrane vesicles (MVs), which are nano-sized bilayered proteolipids (16). Naturally produced MVs are potentially an effective way to deliver toxins, enzymes, and other effectors to host tissues. Additionally, evidence from various studies support that MVs participate in intercellular communication and horizontal gene transfer (16–21). In GC, MVs are necessary for biofilm formation, which is thought to play an important role in asymptomatic infection in women, resistance to antimicrobial agents, and suppression of host immune defenses (22–24). MVs may also contribute to the serum resistance by providing an enhanced ability to bind and eliminate bactericidal factors (17).

Although the potential importance of proteins localized to the GC cell envelope and MVs has been reported previously (25, 26), only two proteomic studies have been published addressing GC membrane composition (27, 28). Most studies have focused on extensive characterization of factors involved in direct host cell interaction: protruding surface proteins (pili), outer membrane adhesins Opa, porins P.IA and P.IB, lipooligosaccharide, and several iron utilization proteins (3, 4, 15, 29–32). Many of these vital virulence factors undergo phase and/or antigenic variation, making them poor drug or vaccine targets. Therefore, the pursuit for novel and constitutively expressed proteins—therapeutic targets in GC—is of utmost importance.

Accordingly, in this study we applied global and unbiased proteomics to compare the composition of both the cell envelopes and MVs isolated from four GC strains: FA1090, F62, MS11, and 1291. Specifically, we used **i**sotope **t**agging for **r**elative and **a**bsolute **q**uantification (iTRAQ) coupled with multidimensional liquid chromatography and tandem mass spectrometry (2D-LC/MS/MS). This approach allowed us to determine a uniformly and differentially expressed repertoire of proteins. Focusing on a homolog of LPS transport protein, LptD (OstA, Imp), which was identified in both the cell envelopes and MVs fractions, and ubiquitously expressed among analyzed strains, we showed that its depletion led to loss of GC viability. Finally, we selected for initial characterization six predicted outer membrane proteins, which were present at similar levels in the GC cell envelopes. We generated Δ*ngo1344*, Δ*ngo1955*, Δ*ngo1985*, Δ*ngo2111*, Δ*ngo2121*, and Δ*ngo2139* mutant strains and examined their sensitivity toward different cell envelope-perturbing agents as well as chloramphenicol. These studies showed that the lack of NGO1985 resulted in dramatically decreased GC viability, suggesting that this protein functions in the maintenance of the cell envelope permeability barrier. Overall, these findings further support our hypothesis that the conserved proteins may represent promising targets for designing new therapeutic interventions.

EXPERIMENTAL PROCEDURES

Bacterial Strains and Growth Conditions—GC strains FA1090, F62, MS11, and 1291 used in this study are described in detail in Table I. Additionally we used strain FA19 (33), and a few isolates (LGB1, LG14, LG20, and LG26) collected from two public health clinics in Baltimore between 1991–1994. The strains were grown on either solid media, GCB agar in 5% CO_2 atmosphere at 37 °C, or in liquid media, GCBL, at 37 °C as previously described (34–36). GCB agar is GC Medium Base agar (Difco, Detroit, MI) with Kellogg's supplements, whereas GCBL is a GC Medium Base broth containing Kellogg's supplements and sodium bicarbonate at a final concentration of 0.042%. For anaerobic growth, GC was grown as described previously in an anaerobic jar using GasPak Plus anaerobic system with palladium catalyst (BD) and indicator strip (BBL) at 37 °C for 24 h in the presence of 5 μl of 20% sodium nitrite spotted on a paper disc placed in the middle of the GCB plates (37, 38).

To examine the proteome of the cell envelope and MVs, GC strains FA1090, F62, MS11, and 1291 were streaked at the same time on GCB plates and incubated for 20 h in 5% CO_2 at 37 °C. Subsequently, bacteria were swabbed from plates and suspended in prewarmed GCBL medium to an optical density at 600 nm (OD_{600}) of 0.1 and cultured in Fernbach flasks with shaking at 220 rpm. Growth was monitored every hour by determining the turbidity of the cultures (OD_{600}). All cultures were harvested at the late-logarithmic phase of growth (at OD_{600} about 0.8). Cells were separated from culture supernatants by low speed centrifugation (6000 × *g*), and both membrane fractions and MVs were prepared for proteomic analysis as described below.

Preparation of the GC Cell Envelope Fraction—Preparation of the cell envelope fraction was accomplished according to (39, 40) with the following modifications. Pellet of bacterial cells obtained from 1.0 L of each GC strain cultured as described above was suspended in phosphate buffered saline pH 7.5, (PBS, Li-Cor, Lincoln, NE) supplemented with Complete Protease inhibitor mixture tablets EDTA-free (buffer A, Roche). Then, GC cells were lysed by three passages through French pressure cell at 12,000 psi, and the unbroken bacterial cells and debris were removed by centrifugation at 7000 × *g* for 30 min at 4 °C. Cell lysates obtained from respective GC cultures were subsequently diluted four times with freshly prepared ice-cold 0.1 M sodium carbonate (pH 11 without adjustment). The suspensions were sonicated (2 × 20 s, 5 Watts) and incubated for 1 h at 4 °C with a gentle stirring. Following another two cycles of sonication (20 s/cycle, 5 Watts), the crude membrane fractions were collected by ultracentrifugation in a Beckman Type 70 Ti rotor at 170,000 × *g*, 1 h, 4 °C. To remove the residual membrane associated proteins, the pellets were washed with ice-cold buffer A, sonicated (3 × 15 s, 5 Watts), and separated at 100,000 × *g*, 2 h, 4 °C in a Beckman SW41Ti rotor. These procedures were repeated twice and finally the pellets containing membrane proteins were suspended in 1 ml of PBS containing 0.2% SDS. The total concentration of proteins in each sample was assessed with 2-D Quant Kit (GE Health Care).

Preparation of Naturally Released MVs—The naturally released MVs were prepared using optimized protocol for GC (18). Briefly, supernatants (about 1.0 L per each culture) obtained from the same GC cultures used for cell envelope extractions, were first passed through the 0.22 μm filter units (ThermoFisher Scientific) and to prevent proteolysis, Complete Protease inhibitor mixture tablet EDTA-free was added. Subsequently, the supernatants were subjected to ultracentrifugation at 210,000 $\times$ *g*, 3 h, 4 °C in a Beckman Type 45 Ti rotor. The pellets containing MVs fraction were washed with PBS and finally reconstituted in PBS containing 0.2% SDS. The total protein concentration in MVs was measured using 2D Quant Kit.

Transmission Electron Microscopy—Native MVs isolated from culture supernatants of GC strains FA1090, F62, MS11, and 1291 as described above, were reconstituted in PBS, adsorbed on a formvar/carbon coated copper grid for 5 min, and stained with 2% ammonium molybdate for 1 min. Grids were air-dried and MVs were observed using FEI Titan 80–200 transmission electron microscope at the Oregon State University Electron Microscopy Facility.

iTRAQ Labeling, Two-Dimensional Liquid Chromatography, and Mass Spectrometry—Proteins obtained from the cell envelopes and MVs extractions (100 μg and 40 μg, respectively) were precipitated overnight at −20 °C in 90% acetone and washed twice with ice-cold acetone. iTRAQ (AB Sciex) labeling was performed according to the manufacturer's recommendations. The following iTRAQ tags were used to label peptides in appropriate GC strains: 114 for FA1090, 115 for F62, 116 for MS11, and 117 for 1291. The reactions were carried out for 1 h at room temperature and were stopped by the addition of 250 μl of 0.1% Trifluoroacetic acid (TFA). Labeled peptides were pooled and purified on C18 column (Honeywell Burdick & Jackson). Subsequent procedures were performed at the Proteomic Core at Fred Hutchinson Cancer Research Center, Seattle, WA. iTRAQ labeled peptides were separated by strong cation exchange (SCX) using a Paradigm MG4 HPLC (Michrom Bioresources/Bruker). Peptide separations were performed using a Zorbax300 SCX column (2.1 mm $\times$ 150 mm; Agilent Technologies, Santa Clara, CA) with an in-line guard cartridge. Peptides were eluted using SCX A and SCX B buffers with a flow rate of 200 μl/min using the following gradient: 2% B from 0 to 5 min, 8% B to 5.1 min, 18% B to 20 min, 34% B to 32 min, 60% B to 40 min, 98% B to 40.1 min and held to 50 min, 2% B to 50.1 min and held to the end of the run at 60 min. SCX A buffer contained 5 mM KH_2PO_4 pH 2.7, 30% (v/v) acetonitrile (ACN) and SCX B buffer contained SCX A buffer with 500 mM KCl. Fractions were collected at 2 min intervals throughout the run and pooled to a reduced number of fractions for reversed-phase (RP-HPLC-MS) analysis based on ultraviolet absorption at 220 nm. The pooled fractions were dried in a vacuum concentrator. Each pooled fraction was reconstituted with 0.1% TFA (100 μl) and desalted using SepPak C18 cartridges (Waters, Milford, MA). Peptides were eluted with 50% ACN/0.1% TFA and concentrated in a vacuum concentrator. Subsequently, peptides were separated using Eksigent nano-two-dimensional high-pressure liquid chromatography (2D HPLC, AB Sciex). In-line de-salting was accomplished using a reversed-phase trap column (100 μm $\times$ 20 mm) packed with Magic C_{18}AQ (5-μm 200 Å resin; Michrom BioResources) followed by peptide separations on a reversed-phase column (75 μm $\times$ 250 mm) packed with Magic C_{18}AQ (5-μm 100 Å resin; Michrom BioResources) directly mounted to the Dionex Probot MALDI Spotter (ThermoFisher Scientific). A 90 min gradient from 7% to 35% ACN in 0.1% TFA at a flow rate of 500 nL/min was used for chromatographic separations. The gradient of solvent B was as follows: 0 min, 5% B; 2 min, 7% B; 92 min, 35% B; 93 min, 50% B; 102 min 50% B; 103 min, 95% B; 108 min, 95% B; 109 min, 5% B; 129 min, 5% B; and 130 min, 5% B. The column effluent was mixed in a micro Tee with matrix (5 mg/ml alpha-cyano 4-hydroxy cinnamic acid (Sigma-Aldrich) with 2% Ammonium Citrate (Sigma-Aldrich) and 40 fmol/μl Glu-Fibrinopeptide B (in-house synthesis) delivered at 1 μl/min. Fractions were spotted at 10 s intervals onto a stainless steel MALDI target plate (AB Sciex). MS and MS/MS spectra were acquired on an Applied Biosystems 4800 Proteomics Analyzer (TOF/TOF) (AB Sciex) in positive ion reflection mode with a 200 Hz Nd:YAG laser operating at 355 nm, and accelerating voltage with 400 ns delay. MS spectra were obtained with minimal laser energy in order to maintain the best resolution. MS spectra for the entire sample set were collected first, and on each sample spot MS/MS spectra were collected for the 20 most intense peaks above the signal-to-noise ratio threshold of 20 using a collision energy of 2 keV and air as the collision gas. Both MS and MS/MS data were acquired on the sample spots using an internal calibration with Glu-Fibrinopeptide B.

Proteomic Data Analysis—Data analysis was performed using the Paradigm search algorithm, which is a part of the ProteinPilot software (version 4.0) (AB Sciex) against the SwissProt target-decoy database for *N. gonorrhoeae* FA1090 with 1963 protein entries (downloaded on January 17, 2012). The user-defined search parameters were selected as follows: Sample Type: iTRAQ 4plex, Cys. Alkylation: MMTS, Digestion: Trypsin, Instrument: 4800, ID Focus: Biological Modifications, Search Effort: Thorough, FDR Analysis: Yes, User Modified Parameter Files: No. All other search parameters, such as number of missed and/or nonspecific cleavages allowed and the mass tolerance of the precursor and fragment ions, are hard-coded into the ProteinPilot software for analyzing MALDI 4800 data. The ProGroup Algorithm built within ProteinPilot software was used to perform the statistical analysis on the identified peptides to determine the minimal set of identifications. Data were normalized by bias correction built in ProteinPilot. The mass spectrometry proteomics data have been deposited in the ProteomeXchange Consortium (http://proteomecentral.proteomexchange.org) via the PRIDE partner repository ProteomeXchange with the dataset identifier PXD000549. The annotated spectra can be examined using MS-Viewer, which is available on the public Protein Prospector website at the following uniform resource locator: http://prospector2.ucsf.edu/prospector/cgi-bin/msform.cgi?form=msviewer. The search keys for the individual data sets are as follows: ikgoxmdesw (cell envelope Exp.1; x5616y5bsg (cell envelope Exp.2); nyiveb6jjz (MVs Exp1); and zv4dvvldqm (MVs Exp. 2). Unprocessed and unfiltered results from Protein Pilot can be found in Microsoft Excel files in the supplemental Material S1–S4. All statistical analyses were performed as we described previously (41). Briefly, only proteins identified with 1% FDR with at least one peptide of 95% confidence or more were recorded. For protein quantification, only proteins with associated *p* values corresponding to the calculated iTRAQ ratios were included. Proteins were considered ubiquitously expressed if the iTRAQ ratios were between 0.5 and 2, and were designated as differentially expressed when the values were below 0.5 or above 2 with the corresponding *p* values $<$ 0.05 in both biological experiments. The relative protein abundance heat maps were constructed using MultiExperiment Viewer (MeV version 4.8) (42).

Bioinformatics Analyses—Subcellular localization of identified proteins was assessed using PSORTb 3.0.2 (43), SOSUIGramN (44), and CELLO 2.5 (45, 46), and majority-votes strategy was used for protein assignment. In cases where PSORTb, SOSUIGramN, and CELLO 2.5 predicted different subcellular localizations for a particular protein, the protein was allocated to a group of "unknown subcellular localization." Furthermore, the predicted amino acid sequences of identified proteins were analyzed for the presence and location of signal peptides cleavage sites using both SignalP v.4.1 (47) and TatP v1.0 (48) servers. To phylogenetically classify identified proteins the Clusters of Orthologous Groups (COGs) functional categories were assigned using COGnitor, WebMGA (49, 50), and J. Craig Venter Institute-Compre-

hensive Microbial Resource (http://cmr.jcvi.org/tigr-scripts/CMR/). The predicted amino acid sequences of selected, newly identified proteins were also analyzed using protein BLAST similarity searches (www.ncbi.nlm.gov.blast).

Genetic Manipulations—The genome sequence of GC strain FA1090 was used as a template to design primers. Chromosomal DNA purified from FA1090 using Promega Wizard Genomic DNA Purification Kit was used in PCR reactions. Reactions were performed using Q5 High-Fidelity DNA Polymerase (New England BioLabs, Ipswich, MA) with oligonucleotides synthesized by Integrated DNA Technologies. PCR products were verified by sequencing at the Center for Genome Research and Biocomputing at OSU. The sequences of all oligonucleotides designed and used in this study are listed in the supplemental Table S1.

Construction of GC Strains Expressing RpsM-His, NGO1985-His, and NGO2054-His From Their Native Chromosomal Loci—Splicing by overlap extension PCR (SOE PCR) (51) was used to engineer an epitope-encoding tail, 6×His-tag, at the 3′ end of individual genes *ngo1821*, *ngo1985*, and *ngo2054* in their respective loci of the FA1090 chromosome. The nucleotide sequence encoding 6×His-tag followed by a stop codon was included within the corresponding oligonucleotides. PCR reactions were used to amplify 500 bp upstream and downstream from the stop codon of each gene. Both fragments were spliced using a set of the external primers. The individual SOE PCR products were used to transform strain FA1090 in liquid culture as described (52). The presence of the His-tag-encoding sequence at the 3′ end of the particular gene was confirmed by PCR reaction using a forward primer specific to the His-tag, NGO-His, and a reverse primer designed to the individual gene; RpsM-His-down-R, NGO1985-His-down-R, or NGO2054-His-down-R.

Construction of Conditional lptD Mutant Strain—The conditional *lptD* mutant strain, FA1090 P_{lac}*lptD*, was constructed as follows. First, a gene encoding LptD (NGO1715) including an upstream region encoding native ribosome binding site was amplified with primers NGO1715-C-F and NGO1715-C-R. The 2422 bp PCR product was subjected to digestion with endonuclease FseI and subcloned into ScaI/FseI-pGGC4, to yield pGCC4-*lptD*, resulting in the placement of the *lptD* gene behind the P_{lac} promoter. This vector uses the Neisserial Complementation System and contains an isopropyl-β-D-thiogalactoside (IPTG)-inducible promoter, thus allowing controlled expression of a cloned gene (53). Subsequently, the fragment containing *lacI* repressor gene, P_{lac} promoter and 630 bp of *lptD* gene was amplified with primers NGO1715-Down-F and NGO1715-Down-R, digested with BamHI and SalI and ligated into pUC18K, creating pUC18K-P_{lac}*lptD* (54). Then the upstream region of *lptD* was amplified using primers NGO1715-Up-F and NGO1715-Up-R. The resulting 516 bp product was digested with EcoRI and KpnI, and cloned into pUC18K-P_{lac}*lptD*. This final construct containing nonpolar kanamycin resistance cassette *apha-3* (54) flanked by homologous regions for recombination and allelic exchange (upstream region of *lptD*, and P_{lac}*lptD*) was used to introduce the mutation onto the FA1090 chromosome. The plasmid was linearized by digestion with NdeI and transformation was conducted as described previously with the exception that the growth media were supplemented with IPTG (100 μM final concentration) (55). Transformants were plated on GCB agar with 40 μg/ml kanamycin and 100 μM IPTG and selected FA1090 P_{lac}*lptD* clones were verified by PCR.

Construction of In-frame Deletion Mutants Δngo1985, Δngo1344, Δngo1955, Δngo2111, Δngo2121, and Δngo2139—All strains containing in-frame deletions of individual genes were constructed using a scheme of genetic manipulations briefly described below. The length of individual PCR products as well as restriction enzymes used in cloning procedures are listed in the supplemental Table S1. The upstream regions of particular genes (about 500 bp) were amplified with primers designated as NGO-up-F and NGO-up-R (where F-forward and R-reverse). Subsequently, PCR products were digested and cloned into pUC18K vector, yielding pUC18K-*ngo*-up. Similarly, the corresponding downstream regions of individual genes (about 500 bp) were first amplified using primers NGO-down-F and NGO-down-R. The resulting PCR products were subjected to digestion with appropriate restriction enzymes and cloned into pUC18K-*ngo*-up. Thus, these final constructs, pUC18K-Δ*ngo*, contained kanamycin resistance cassette (54) flanked by homologous regions for recombination and allelic exchange. The specific pUC18K-Δ*ngo* was linearized with NdeI and transformation of GC was conducted as described (55). The presence of desired mutation on the FA1090 chromosome was examined with respective primers listed in the supplemental Table S1. In all PCR reactions, chromosomal DNA isolated from wild-type bacteria was used as a control.

To Construct the Complemented Strain, Δ*ngo1985*/P_{lac}*ngo1985*, first, the 643 bp fragment of *ngo1985* with a native ribosome-binding site was amplified with primers NGO1985-C-F and NGO1985-C-R. The PCR product was subjected to digestion with endonuclease FseI and subcloned into ScaI/FseI-pGGC4, to yield pGCC4-P_{lac} *ngo1985*, which was subsequently used to complement the Δ*ngo1985* strain as described above.

Effect of LptD Depletion on GC Physiology—To examine the effect of LptD depletion on GC physiology, FA1090 P_{lac}*lptD* were plated from freezer stocks onto GCB plates supplemented with 100 μM IPTG. The following day, single nonpiliated colonies were passaged onto fresh GCB plates containing 100 μM IPTG and incubated ~18 h in 5% CO_2 atmosphere at 37 °C. A sterile Dacron swab was used to collect the bacteria from plates and suspend them to OD_{600} = 0.1 in a prewarmed to 37 °C GCBL. After three washes in GCBL, bacteria were divided and cultured in the presence or absence of IPTG (as indicated) for 5 h with shaking (220 rpm) at 37 °C in GCBL. Bacterial growth was monitored every hour by both measuring absorbance at OD_{600} and assessing cell viability by spotting 10 μl of 10-fold serial dilutions of GC cultures onto GCB agar plates with or without IPTG. The number of colonies was examined after 22 h, and colony-forming units, CFU, were calculated per ml of bacterial culture. These experiments were performed on four separate occasions and mean values and standard deviations of the mean (S.E.) are presented. Bacterial colonies were visualized with a Zeiss AxioObserver.D1 microscope at A-Plan 10× magnification 0.25 P hase Contrast 1.

Phenotypic Analysis of Knockout Strains for Sensitivity to Different Chemical Probes—The individual knockout strains Δ*ngo1985,* Δ*ngo1344,* Δ*ngo1955,* Δ*ngo2111,* Δ*ngo2121,* and Δ*ngo2139*, the complemented strain Δ*ngo1985*/P_{lac}*1985*, as well as isogenic parent strain, FA1090, were plated from freezer stocks and nonpiliated colonies were passaged as described above. All GC strains were collected from plates, and suspended to 5×10^5 CFU/ml in a prewarmed to 37 °C GCBL supplemented with 100 μM IPTG. Subsequently, 10 μl of undiluted and 10-fold serial dilutions of cell suspensions were spotted on solid media containing 100 μM IPTG and with or without the addition of various compounds (as indicated in the text). Bacterial growth was examined after 22 h. The relative viability of each GC strain was calculated by comparing CFUs/ml on GCB plates supplemented with different chemicals to the CFUs/ml on control plates. These experiments were performed in biological triplicates and mean values with calculated S.E. are presented.

Purification of Recombinant Soluble Domain of AniA and Generation of Rabbit Polyclonal Antibody—The gene encoding AniA (NGO1276) lacking the N-terminal palmitoylation signal was amplified, cloned, and purified as described previously in a study by Boulanger *et al.*, where the three-dimensional crystal structure of AniA was resolved (56). Subsequently, 3 mg (1 mg/ml) of purified, recombinant soluble form of AniA was submitted to Pacific Immunology

TABLE I
Summary of recognized differences between GC isolates utilized in this study

Characteristic	FA1090	F62	MS11	1291	Reference
Source	DGI[a]	Urethra	Endocervix	Urethra	(30)
Serum susceptibility	Resistant	Sensitive	Sensitive	Intermediate	(30, 57, 107, 108)
Genetic island	Absent	Absent	Present	Present	(109)
Iron utilization[b]	Tbp+, Lf−	Tbp+, Lf−	Tbp+, Lf+	n/a	(110)

[a] DGI–Disseminated GC Infection.
[b] Tbp–Transferrin binding protein; Lf–Lactoferrin binding protein; (+) – present; (−) - absent.

Corporation, where it was used to immunize two rabbits to generate polyclonal antibodies.

SDS-PAGE, Coomassie Staining and Immunoblotting Analyses—Cell envelopes, MVs, and cytoplasmic proteins were extracted from GC strains as described in the sections above. Whole cell lysates were derived from GC grown on GCB plates either anaerobically or aerobically, as specified in the text. When bacterial colonies reached approximately the same size, all strains were harvested, suspended in prewarmed GCBL, and the cell density was assessed turbidometrically at OD_{600}. Cytoplasmic proteins, cell envelopes, and MVs (15 μg of proteins loaded per lane), or whole cell lysates matched by equivalent OD_{600} units, were boiled in SDS sample buffer in the presence of 50 mM dithiotreitol and resolved in 4–20% Tris-glycine gradient gels (Bio-Rad, Hercules, CA). When indicated, purified recombinant AniA (250 ng) was loaded as a positive control. The gels were either stained with Colloidal Coomassie Blue G-250, and imaged using GelDoc MP (Bio-Rad) or subjected to electrotransfer of proteins onto 0.2 μm nitrocellulose membrane (Bio-Rad) using Trans-blot Turbo (Bio-Rad). The membranes were blocked in 5% milk in PBS supplemented with 0.1% Tween 20, followed by incubation with polyclonal rabbit antisera against either AniA (1:5000) or Ng-MIP (1:10,000), monoclonal mouse antisera against MtrE (1:1000), or monoclonal mouse antibody against 6×His epitope tag (1:1000; ThermoFisher Scientific). The horseradish peroxidase conjugate of either goat anti-rabbit IgG antibody (BioRad) or goat anti-mouse IgG antibody (ThermoFisher Scientific) was used as secondary antisera at 1:10,000 dilution. Immunoblots were developed using Clarity Western ECL-Substrate (BioRad) on Chemi-Doc™ MP System (BioRad).

RESULTS AND DISCUSSION

Rationale and Experimental Design—To identify the potential target proteins for development of new pharmacological interventions against GC infections, we compared the proteomes of cell envelopes and MVs derived from four GC isolates: FA1090, F62, MS11, and 1291. We chose these strains for the following reasons: (1) they display several notable differences that might contribute to their fitness in a human host including resistance to human serum, ability to use iron from human transferrin and lactoferrin for growth, and presence of the GC genetic island (Table I) (30, 34, 57–61); (2) their genomes have been sequenced (62); and (3) they have been used in many laboratories and human volunteer studies over the past 20 years (61).

Our experimental design for profiling of the GC cell envelope and MVs is outlined in Fig. 1. Bacterial cultures (1.0 L volume) of FA1090, F62, MS11, and 1291 were propagated simultaneously under standard laboratory growth conditions as described under "Experimental Procedures." The culture supernatants containing naturally elaborated MVs were separated from bacterial cells by low speed centrifugation at the late-logarithmic phase of growth (Fig. 1*A*). This stage of growth has been proven for GC to accumulate native MVs (17). Subsequently, cell pellets were used for isolation of membrane proteins by a sodium carbonate extraction procedure (40). This method facilitates efficient enrichment of membrane proteins and ensures the suitability of the samples for mass spectrometry analysis (39, 40, 63). To provide enough material for proteomic analyses of MVs, the entire amount of each cell-free culture supernatant (about 1.0 L) was filtered to remove any remaining bacterial cells and subjected to ultracentrifugation using optimized protocol for GC (18). Transmission electron microscopy of the harvested MVs fractions demonstrated the presence of spherical, tubular, and lobed MVs with wide variation in dimensions (Fig. 1*B*). Similar morphological types of MVs released by GC were reported previously (64). The examination of the purified cell envelopes and MVs by 1 D SDS-PAGE revealed, as expected, the presence of common and distinct proteins, and the differences were particularly apparent in the MVs fraction (Fig. 1*C*). The most prominent proteins migrated at about 35 and 25 kDa, likely corresponding to the GC major porins PorIB (P.IB) and PorIII, respectively (65, 66).

Comprehensive identification of cell envelope and MVs proteins represents a challenge because they are commonly hydrophobic, have a basic charge, and are often of high molecular weight. Thus, it is widely accepted that two-dimensional gel electrophoresis has very limited capabilities for the separation of integral membrane proteins (21, 67). Instead, a multidimensional protein identification technology that separates proteins using a combination of two different kinds of liquid chromatography (2D-LC) prior to protein identification significantly reduces the complexity of the sample at the peptide level, resulting in the identification of a greater number of proteins. Accordingly, we used a comprehensive proteomic platform including iTRAQ coupled with 2D-LC/MS/MS to identify and quantitatively compare proteins in both the GC cell envelope and naturally elaborated MVs. This proteomic approach allows for simultaneous comparison of up to eight samples of complex protein mixtures (68). In a four-plex experiment, proteins in each sample are subjected to digestion by trypsin or other proteolytic enzymes, and the obtained peptides are labeled at their free amine group with one of the four available mass tag labels: 114, 115, 116, and 117 (Fig.

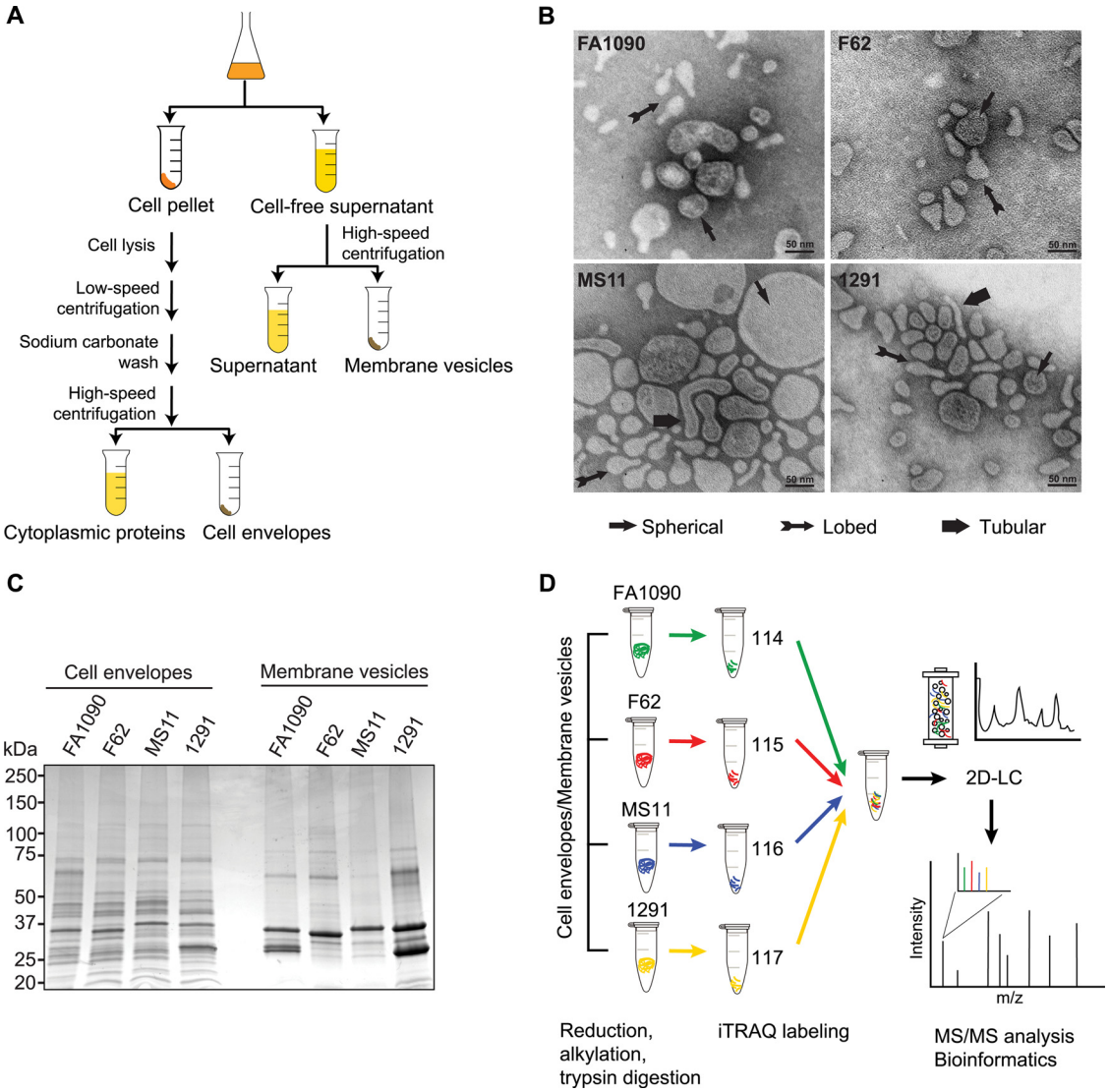

FIG. 1. **Flowchart describing the proteomic strategy for a discovery of potential therapeutic targets in GC.** *A*, Workflow of preparation cell envelopes and MVs from GC strains: FA1090, F62, MS11, and 1291. Strains were cultured aerobically in GCBL medium at 37 °C to reach OD_{600} = 0.8. Bacterial cells and culture supernatants were separated by low-speed centrifugation. Subsequently, cells were lysed and the crude membrane fractions were obtained by cold sodium carbonate extraction at high alkaline pH and ultracentrifugation steps. Cell-free culture supernatants were subjected to high-speed centrifugation at 210,000 × *g* for 3 h to pellet MVs. *B*, Native MVs purified from strains FA1090, F62, MS11, and 1291 were negatively stained, and visualized by transmission electron microscopy. The different morphological classes of MVs, indicated by arrows, included spherical, lobed, and tubular. *C*, Profiles of isolated GC cell envelopes and MVs proteins. Cell envelopes and MVs fractions were prepared from aerobically grown cultures of strains FA1090, F62, MS11, and 1291. Samples were normalized by the total protein concentration and 15 μg were loaded per lane of 1D SDS-PAGE 4–20% Tris-glycine gel. Proteins were visualized by staining with Colloidal Coomassie Blue G250. The migration of molecular weight markers and their masses in kilodaltons (kDa) are indicated on the left. *D*, Outline of four-plex iTRAQ labeling coupled with 2D-LC/MS/MS. The total amounts of 100- and 40-μg of the cell envelope and MVs proteins, respectively, were reduced, alkylated, and trypsinized. The following iTRAQ tags were used to subsequently label peptides derived from respective GC strains: 114 for FA1090, 115 for F62, 116 for MS11, and 117 for 1291. After labeling the samples were pooled and subjected to SCX fractionation followed by a reversed-phase separation (2D-LC) and protein identification, and quantification using MALDI-TOF MS/MS. Integrated bioinformatics and statistical analyses were applied including ProteinPilot software.

1*D*). While, in an eight-plex experimental approach, in addition to the latter tags, 113, 118, 119, and 121 are also used. Comparison of the intensity of these reporter labels permits the relative quantification of identical peptides in each digest and thus the proteins from which they originate (68). In our studies, the four-plex iTRAQ was used on two separate occasions to label either 100 or 40 μg of cell envelope or MVs proteins, respectively, obtained from each GC strain (Fig. 1*D*). Thus, four independent iTRAQ experiments were performed in total. The following iTRAQ tags were used for respective GC strains: 114 for FA1090, 115 for F62, 116 for MS11, and 117 for 1291. After labeling, the samples were pooled and sub-

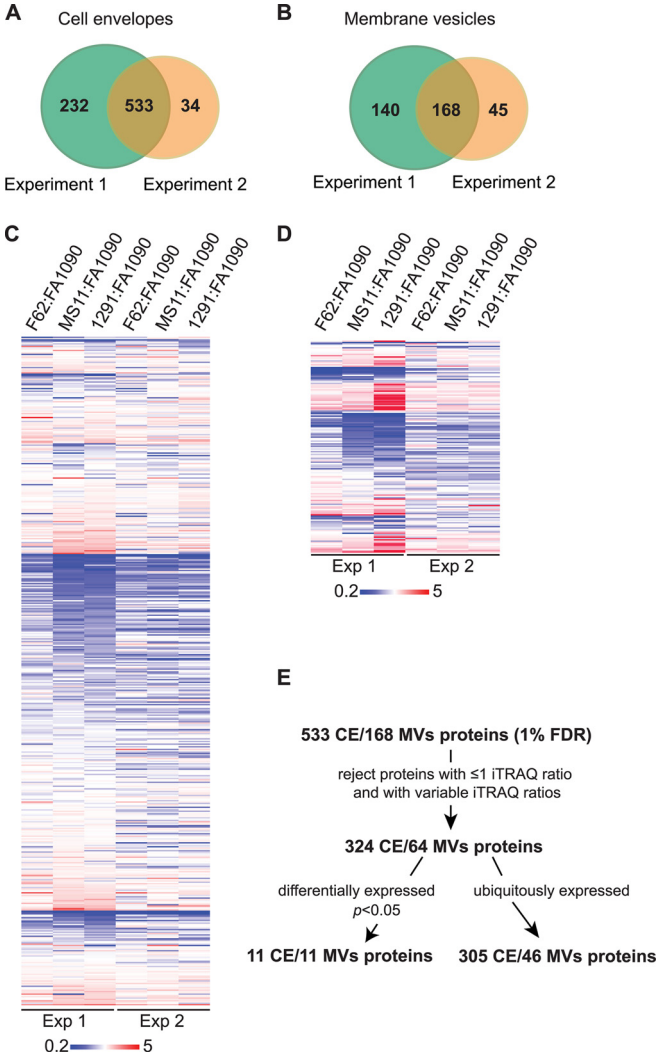

FIG. 2. **Quantitative proteomics profiling of the cell envelopes and MVs isolated from GC strains FA1090, MS11, F62, and 1291.** *A,* Venn diagram of proteins identified in the cell envelopes in biological replicate experiments. A total of 765 and 567 individual protein species was identified in Experiment 1 and 2, respectively. *B,* Distribution of proteins identified in MVs in two independent experiments (Experiments 1 and 2). A total number of 308 and 213 proteins was identified, respectively. *C,* and *D*, Heat maps illustrating the relative abundance of common proteins identified in both biological experiments in the cell envelopes and MVs, respectively. To quantify the abundance of the proteins, strain FA1090 was arbitrarily chosen as the reference strain. The color scale covers fivefold down-regulation (blue), via no change (white), to fivefold up-regulation (red). *E*, Flowchart outlining the strategy for rigorous analysis of data obtained during proteomic profiling of the GC cell envelopes (CE) and MVs.

jected to SCX fractionation followed by a reversed-phase separation and protein identification, and quantification using MALDI-TOF MS/MS (Fig. 1*D*).

Strategy for Rigorous Proteomic Profiling of the GC Cell Envelopes and MVs—The proteome mining of the GC cell envelopes revealed 765 and 568 proteins in two independent iTRAQ experiments (Fig. 2*A* and supplemental Table S2). Further, 308 and 213 proteins were detected in the MVs fractions (Fig. 2*B* and supplemental Table S3). All of these proteins were identified with <1% false discovery rate. There were 533 and 168 common proteins in the cell envelopes and MVs, respectively, identified in all four GC strains in both proteomic studies (Fig. 2*A* and 2*B*).

To quantify the relative abundance of identified proteins, strain FA1090 was arbitrarily selected as the reference strain and the iTRAQ ratios were calculated as follows: F62/FA1090 (115/114), MS11/FA1090 (116/114), and 1291/FA1090 (117/114). Similarly to our previous study (41) a >2.0-fold change in the iTRAQ ratios was chosen as a criterion for differential protein abundance (Fig. 2*C* and 2*D*). Subsequently, proteins without associated iTRAQ ratios, quantified in only one experiment, and displaying variable reporter ratios were eliminated (Fig. 2*E*). Hence, only these proteins were considered, which in two independent experiments were consistently identified as either ubiquitously (iTRAQ ratios of 0.5<proteins<2) or differentially expressed (down- and up-regulated with calculated $p < 0.05$ and the reporters ratios of either <0.5 or >2, respectively). This rigorous strategy eliminated nearly 40 and 68% of proteins identified in the cell envelope and MVs fractions, and the total number of quantified protein species decreased to 316 and 57, respectively (Fig. 2*E*, Tables II–V and supplemental Tables S4–S5). These proteins were subjected to further computational analysis.

Bioinformatic Analyses—Coupling bioinformatics prediction with experimental subcellular proteomics is particularly important because cytoplasmic proteins are repeatedly identified as constituents of the cell envelopes and MVs in both Gram-negative and Gram-positive bacteria (21, 63, 67, 69–71). Many of the cytoplasmic proteins co-purify as components of large protein complexes that are localized to the membrane, whereas others are likely present as a function of cell lysis occurring during culture (63). We reasoned that the latter group might be higher in autolytic bacteria like GC (13). To analyze the subcellular distribution of identified proteins, a combination of bioinformatics tools was used including PSORTb, CELLO 2.5, and SOSUIGramN (43–46). A majority-votes strategy was chosen for the cellular assignment of proteins, and in these cases where the three engines assigned different localizations, a particular protein was allocated to a group of "unknown subcellular localization." Additionally, SignalP and TatP servers were employed to analyze the predicted amino acid sequences of individual proteins for the presence of either N-terminal signal peptide (47) or specifically Twin-arginine signal peptide cleavage sites (48), respectively (Tables II–V). These analyses revealed that in the cell envelope fractions the total numbers of 1, 21, 43, 45, 171, and 43 proteins were localized either extracellularly, to the outer membrane, periplasm, inner membrane, cytoplasm, or unknown, correspondingly (Tables II and IV, and supplemental Table S4). The predicted subcellular distribution of proteins identified in the MVs fraction was as follows: 9-outer mem-

TABLE II
Ubiquitous proteins identified by iTRAQ in the GC cell envelope

Accession	Name	Gene	Average ratio ± S.D.[a]			S[b]	T[c]
			F62:FA1090	MS11:FA1090	1291:FA1090		
Extracellular							
Q5F7V4	Lipoprotein	NGO1063	1.31 ± 0.26	1.45 ± 0.17	1.18 ± 0.1	Y	N
Outer membrane							
Q5F5F6	Adhesin mafA 1/4	mafA1/NGO1067 mafA4/NGO1972	0.63 ± 0.03	1.1 ± 0.01	1.47 ± 0.32	N	N
Q5F9W0	Competence lipoprotein	bamD, comL/NGO0277	1.07 ± 0.09	1.25 ± 0.39	1.06 ± 0.02	Y	N
Q5F679	Efflux pump protein, fatty acid resistance	emrA/NGO1683	1.33 ± 0.22	0.98 ± 0.3	1.42 ± 0.11	N	Y
Q5F651	LPS-assembly protein LptD	lptD, imp, ostA/NGO1715	1.14 ± 0.19	1.34 ± 0.29	1.23 ± 0.1	Y	N
Q5F6J5	OmpA/MotB domain-containing protein	NGO1559	1.33 ± 0.2	1.64 ± 0.31	1.1 ± 0.16	Y	N
Q5F5W8	Outer membrane protein assembly factor BamA	bamA/NGO1801	1.27 ± 0.21	1.15 ± 0.39	1.16 ± 0.03	Y	N
Q5F6I1	Outer membrane protein PIII	rmp/NGO1577	1.22 ± 0.27	1.22 ± 0.17	0.73 ± 0.02	Y	N
Q5F7A4	Nitrite reductase[d]	aniA/NGO1276	1.46 ± 0.26	1.15 ± 0.24	1.13 ± 0.31	Y	Y
Q5F8E4	Periplasmic protein	NGO0834	1.49 ± 0.14	1.16 ± 0.09	0.8 ± 0.07	Y	N
Q5F7F3	Peptidyl-prolyl cis-trans isomerase Ng-MIP[e]	mip/NGO1225	1.15 ± 0	0.94 ± 0.09	1.17 ± 0.07	Y	Y
Q5F6Q7	Phospholipase	pldA/NGO1492	1.42 ± 0.14	1.37 ± 0.01	1.15 ± 0	N	N
Q5FAG7	Pilus-associated protein	pilC/NGO0055	1.13 ± 0.04	1.14 ± 0.1	1.21 ± 0.14	N	Y
Q5FAC9	Putative pilus assembly protein	pilN/NGO0097	1.01 ± 0.05	1.13 ± 0.06	1.31 ± 0.03	N	N
Q5F7H3	Putative TonB-dependent receptor protein	NGO1205	0.88 ± 0.04	1.11 ± 0.03	0.67 ± 0.13	Y	N
Q5F518	Putative uncharacterized protein	NGO2121	0.69 ± 0.05	1.14 ± 0.09	0.83 ± 0.06	Y	N
Q5F526	Putative uncharacterized protein	NGO2111	1.08 ± 0.18	0.82 ± 0.04	0.81 ± 0.01	N	Y
Q5F5E4	Putative uncharacterized protein	NGO1985	0.88 ± 0.06	1.17 ± 0.01	0.83 ± 0.04	N	N
Q5F5H0	Putative uncharacterized protein	NGO1956	1.18 ± 0.08	1.4 ± 0.17	1.41 ± 0.02	N	N
Q5F5H1	Putative uncharacterized protein	NGO1955	1.2 ± 0.1	1.15 ± 0.24	1.15 ± 0.1	N	N
Q5F743	Putative uncharacterized protein	NGO1344	1.01 ± 0.05	1.05 ± 0.14	0.9 ± 0.11	N	N
Q5FAD2	Type IV pilus biogenesis and competence protein pilQ	pilQ, omc/NGO0094	1.12 ± 0.19	1.15 ± 0.09	0.89 ± 0.13	Y	N
Periplasmic							
Q5F601	Catalase	katA/NGO1767	0.92 ± 0.05	1.09 ± 0.39	0.97 ± 0.05	N	N
Q5F544	Ferric enterobactin periplasmic binding protein	fetB/NGO2092	1.06 ± 0.06	0.99 ± 0.33	1.27 ± 0.09	N	N
Q5F581	Genome-derived Neisserial antigen 33	NGO2048	1.38 ± 0.21	1.24 ± 0.01	1.28 ± 0.04	Y	N
Q5F809	Lipid modified azurin protein	azu/NGO0994	1.09 ± 0.24	1.07 ± 0.04	1.15 ± 0.01	Y	Y
Q5F765	Lipoprotein	NGO1321	1.14 ± 0.25	1 ± 0.32	1.1 ± 0.08	N	N
Q5F848	Lipoprotein	NGO0948	1.47 ± 0.21	1.34 ± 0	1.05 ± 0.02	N	N
Q5F8T2	Lipoprotein	NGO0678	1.08 ± 0.22	0.99 ± 0.05	0.78 ± 0.09	Y	N
Q5F8W2	Membrane lipoprotein	NGO0648	1.47 ± 0.12	1.02 ± 0	1.43 ± 0.21	N	N
Q5FAC7	Penicillin-binding protein 1A	mrcA/NGO0099	1.46 ± 0.14	0.7 ± 0	0.82 ± 0.01	N	N
Q5F9Z6	Periplasmic protein	NGO0238	1.1 ± 0.04	1.23 ± 0.07	1.31 ± 0.15	Y	N
Q5F9M1	Putative ABC transporter, periplasmic binding protein, amino acid	NGO0372	0.85 ± 0.05	0.97 ± 0.1	1.04 ± 0	Y	Y
Q5F6Q5	Putative ABC transporter, periplasmic binding protein, polyamine	NGO1494	0.79 ± 0.02	0.74 ± 0	1.24 ± 0.03	Y	N
Q5F7C5	Putative ABC transporter, periplasmic binding protein, polyamine	NGO1253	1.14 ± 0.02	0.93 ± 0.2	1.79 ± 0.01	N	N
Q5FA28	Putative ABC transporter, periplasmic binding protein, polyamine	NGO0206	0.64 ± 0	0.83 ± 0.01	1.5 ± 0.12	Y	N
Q5F574	Putative ABC transporter, thiamine-binding periplasmic protein	NGO2056	1.43 ± 0.29	0.84 ± 0.23	1.41 ± 0	Y	N
Q5FAB9	Putative carboxypeptidase, penicillin binding protein	pbp3/NGO0107	1.05 ± 0.28	1.43 ± 0.18	0.83 ± 0.17	Y	N
Q5F718	Putative cytochrome c oxidase subunit	NGO1371	1.15 ± 0.17	1.1 ± 0.46	1.01 ± 0.12	N	N
Q5F598	Putative cytochrome C1	NGO2031	1.16 ± 0.01	1.3 ± 0.01	1.66 ± 0.04	Y	N
Q5F8Y3	Putative murein hydrolase	mltB/NGO0626	1.4 ± 0.06	1.43 ± 0.01	1.05 ± 0.16	Y	N
Q5FA91	Putative serine protease	NGO0138	1.06 ± 0.11	0.98 ± 0.4	1.11 ± 0.06	Y	N
Q5F515	Putative thioredoxin	NGO2124	0.9 ± 0.05	1.02 ± 0.18	1.12 ± 0.04	N	N
Q5F5C7	Putative uncharacterized protein	NGO2002	1.29 ± 0	1.06 ± 0.07	1.34 ± 0.23	N	N
Q5F6P4	Putative uncharacterized protein	NGO1505	1.18 ± 0.11	1.28 ± 0.14	1.71 ± 0.08	N	N
Q5F7W0	Putative uncharacterized protein	NGO1056	1.17 ± 0.15	1.18 ± 0.45	0.95 ± 0.07	N	Y
Q5F7X1	Putative uncharacterized protein	NGO1044	0.94 ± 0.41	1.02 ± 0.11	1.27 ± 0.1	N	N
Q5F7X2	Putative uncharacterized protein	NGO1043	1.07 ± 0.01	1.06 ± 0.2	0.84 ± 0.11	Y	N
Q5F8C4	Putative uncharacterized protein	NGO0861	1.17 ± 0.19	1.4 ± 0.42	1.23 ± 0.16	Y	N
Q5F571	Putativeptide methionine sulfoxide reductase	msrAB, pilB/NGO2059	1.36 ± 0.31	1.19 ± 0.36	1.29 ± 0.33	Y	N
Q5F649	Thiol:disulphide interchange protein	dsbA/NGO1717	0.98 ± 0.02	1.14 ± 0.13	1.28 ± 0.02	Y	Y
Q5F6V7	Thiol:disulphide interchange protein	dsbC/NGO1438	1.37 ± 0.03	1.01 ± 0.1	1.03 ± 0.1	Y	N
Q5F505	Transglycosylase	NGO2135	1.62 ± 0.22	1.29 ± 0.17	0.98 ± 0.12	Y	N
Q5F912	Type IV pilus assembly protein	pilF/NGO0595	1.3 ± 0.1	1.01 ± 0.09	1.07 ± 0.08	N	N
Inner membrane							
Q5F4Z4	ATP synthase subunit b	atpF/NGO2146	1.23 ± 0.03	1.04 ± 0	1.17 ± 0.18	N	N
Q5F9L1	ATP-dependent zinc metalloprotease FtsH	ftsH/NGO0382	1.04 ± 0.05	1.14 ± 0.42	1.29 ± 0.03	N	N
Q5F6M1	Cell division protein FtsQ	ftsQ/NGO1530	0.95 ± 0.05	0.7 ± 0.3	1.01 ± 0.09	N	N

Table II —*continued*

Accession	Name	Gene	Average ratio ± S.D.[a]			S[b]	T[c]
			F62:FA1090	MS11:FA1090	1291:FA1090		
Q5F6L1	Division cell wall protein	dcaA/NGO1540	0.97 ± 0.09	0.88 ± 0.16	1 ± 0.06	N	N
Q5F8I5	Genome-derived Neisseria antigen 1220	NGO0788	1.43 ± 0.03	1.27 ± 0	1.52 ± 0	N	N
Q5F573	Integral membrane protein	NGO2057	1.28 ± 0.09	1.32 ± 0.02	1.26 ± 0.02	N	N
Q5F5L3	Integral membrane protein	NGO1910	0.82 ± 0.06	1.1 ± 0.14	0.94 ± 0.03	Y	N
Q5F795	Integral membrane protein	NGO1288	1.15 ± 0.02	1.06 ± 0.02	1.27 ± 0.03	N	N
Q5F4X8	Lipid A export ATP-binding/permease protein MsbA	msbA/NGO2165	1.07 ± 0.02	1.05 ± 0.16	1.13 ± 0.11	N	N
Q5F6V6	Macrolide export ATP-binding/permease protein MacB	macB/NGO1439	1.25 ± 0.14	0.94 ± 0.4	0.85 ± 0.09	N	N
Q5F4W6	Membrane protein insertase YidC	yidC/NGO2178	1.2 ± 0.07	0.99 ± 0.05	1.2 ± 0.03	N	N
Q5F6K9	Penicillin-binding protein 2	penA/NGO1542	1.15 ± 0	0.79 ± 0.21	1 ± 0.1	N	N
Q5F7H2	Phosphatidylserine decarboxylase proenzyme	psd/NGO1206	1.09 ± 0.02	1.31 ± 0.3	1.32 ± 0.04	N	N
Q5F693	Pilus assembly protein	pilG/NGO1669	1.33 ± 0.05	1.17 ± 0	1.44 ± 0.01	N	N
Q5FAD0	Pilus assembly protein	pilO/NGO0096	1.28 ± 0.15	1.03 ± 0.21	1.35 ± 0.11	N	N
Q5F6W9	Probable ubiquinone biosynthesis protein UbiB	ubiB/NGO1424	1.26 ± 0.1	1.18 ± 0.13	1.39 ± 0.18	N	Y
Q5FA43	Protein translocase subunit SecD	secD/NGO0189	1.24 ± 0.07	1.08 ± 0	1.21 ± 0.11	N	N
Q5F567	Putative 1-acyl-SN-glycerol-3-phosphate acyltransferase	nlaB/NGO2069	1.03 ± 0.08	1.06 ± 0.2	1.48 ± 0.06	N	N
Q5F523	Putative ABC transporter, ATP-binding protein	NGO2116	0.98 ± 0.03	1.12 ± 0.24	1.27 ± 0.05	N	N
Q5F634	Putative ABC transporter, ATP-binding protein	NGO1732	1.22 ± 0.06	1.23 ± 0.03	1.5 ± 0.05	N	N
Q5F969	Putative acyl-CoA ligase	NGO0530	1.13 ± 0.11	1 ± 0.39	1.02 ± 0.06	N	N
Q5F7V3	Putative carbon starvation protein	cstA/NGO1064	1.01 ± 0.04	1.44 ± 0.02	1.55 ± 0.02	N	N
Q5F823	Thiol:disulfide interchange protein DsbD	dsbD/NGO0978	1.11 ± 0.04	1.1 ± 0.21	1.06 ± 0.12	N	N
Q5F952	Putative dnaJ-family protein	NGO0551	1.29 ± 0.23	0.93 ± 0.35	1 ± 0.12	N	N
Q5F7Y5	Putative ferredoxin	NGO1026	0.99 ± 0	0.89 ± 0.03	1.02 ± 0.04	N	Y
Q5F7V7	Putative fimbrial assembly protein	fimB/NGO1060	1.14 ± 0.03	1.01 ± 0.04	1.35 ± 0.09	N	Y
Q5F916	Putative ftsK-like cell division/stress response protein	NGO0590	1.07 ± 0.02	0.98 ± 0.19	1.04 ± 0.08	N	N
Q5F8K3	Putative lipoprotein releasing system transmembrane protein	NGO0769	1.19 ± 0.11	1.17 ± 0.12	1.43 ± 0.05	N	N
Q5F9U8	Putative Na^+/H+ antiporter	NGO0291	1.29 ± 0.2	1.2 ± 0.29	1.53 ± 0.02	N	N
Q5F6S7	Putative NADP transhydrogenase, alpha subunit	NGO1470	1.38 ± 0.01	1.14 ± 0.03	1.26 ± 0.02	N	N
Q5F7A5	Putative nitric oxide reductase	NGO1275	1.5 ± 0.16	1.03 ± 0.05	1 ± 0.19	N	N
Q5F8S5	Putative P-type cation-transporting ATPase	NGO0685	1.03 ± 0	1.22 ± 0.03	1.39 ± 0.02	N	N
Q5F7D2	Putative serine protease	NGO1246	1.46 ± 0.29	0.85 ± 0.17	0.87 ± 0	N	N
Q5FAG5	Putative thioredoxin	NGO0057	1.26 ± 0.09	1.13 ± 0.24	1.12 ± 0.11	N	N
Q5F614	Putative uncharacterized protein	NGO1752	1.14 ± 0.11	1.15 ± 0.34	0.73 ± 0.1	N	N
Q5FA44	Putative uncharacterized protein	NGO0188	1.04 ± 0.08	1.45 ± 0.35	1.32 ± 0.25	N	N
Q5F5W9	RIP metalloprotease RseP	rseP/NGO1800	1.02 ± 0.03	0.95 ± 0.12	1.03 ± 0.1	N	N
Q5F5K7	Transmembrane transporter	NGO1917	0.91 ± 0.12	1.25 ± 0.21	1.28 ± 0.59	N	N
Q5F711	Transport protein	exbB/NGO1378	1.05 ± 0.03	0.82 ± 0.2	0.99 ± 0	N	N
Q5F5Q0	Two-component system sensor kinase	NGO1867	1.12 ± 0.01	1 ± 0.14	1.23 ± 0.03	N	N
Q5FA56	Two-component system sensor kinase	NGO0176	1.14 ± 0.01	1.13 ± 0.08	1.26 ± 0.02	N	N
Q5FAA1	UPF0761 membrane protein NGO0127	NGO0127	1.26 ± 0.14	1.14 ± 0.1	1.07 ± 0.2	N	N
Q5F9N3	Uroporphyrin-III C-methyltransferase	hemX/NGO0360	0.9 ± 0.02	0.86 ± 0.15	1.22 ± 0.1	N	N
Q5F7H9	YhbX/YhjW/YijP/YjdB family protein	NGO1198	1.06 ± 0.09	1.18 ± 0.29	1.12 ± 0	N	N
Unknown							
Q5F8Z8	1-acyl-SN-glycerol-3-phosphate acyltransferase	plsC/NGO0611	1.36 ± 0.11	1.32 ± 0.02	1.5 ± 0.22	N	Y
Q5F5V0	30S ribosomal protein S11	rpsK/NGO1820	1.14 ± 0.03	0.99 ± 0.06	0.92 ± 0.06	N	Y
Q5F913	4-hydroxy-3-methylbut-2-en-1-yl diphosphate synthase	ispG/NGO0594	0.82 ± 0.08	0.67 ± 0.08	0.63 ± 0.09	N	N
Q5F9Z8	Cell division protein zipA	zipA/NGO0236	0.99 ± 0.01	1.11 ± 0.05	1.25 ± 0.01	N	N
Q5F501	Genome-derived Neisserial antigen 1946	NGO2139	1.21 ± 0.04	1.23 ± 0.05	1.74 ± 0.03	Y	Y
Q5F9N2	HemY protein	hemY/NGO0361	1.12 ± 0.03	1.15 ± 0.06	1.29 ± 0.03	N	N
Q5F9W2	IgA-specific metalloendopeptidase	iga/NGO0275	0.93 ± 0.03	1.39 ± 0.1	1.05 ± 0	Y	N
Q5F5I3	Lipoprotein	NGO1942	0.99 ± 0.05	1.24 ± 0.06	1 ± 0.02	N	N
Q5F8J5	Membrane protein	NGO0778	1.12 ± 0.01	0.89 ± 0.27	1.01 ± 0.06	N	N
Q5F7J8	Minor pilin ComP	comP/NGO1177	1.17 ± 0.2	0.62 ± 0.33	1.54 ± 0.01	N	N
Q5F521	Outer membrane transporter	NGO2118	0.96 ± 0.2	1.07 ± 0.21	1.05 ± 0.15	N	N
Q5F8S7	Periplasmic protein	NGO0683	1.04 ± 0.4	0.84 ± 0.08	0.87 ± 0.28	Y	N
Q5FAD1	Pilin assembly protein	pilP/NGO0095	1.19 ± 0.04	1.08 ± 0.07	1.45 ± 0.16	Y	N
Q5F4Y0	Putative 3-oxoacyl-[acyl-carrier protein] reductase	fabG/NGO2163	0.62 ± 0.11	0.8 ± 0.21	0.76 ± 0.02	N	Y
Q5FA61	Putative ABC transporter, ATP-binding protein	znuC, troB/NGO0170	0.87 ± 0.2	0.77 ± 0.23	0.7 ± 0.13	N	N
Q5F531	Putative adhesion and penetration protein	NGO2105	1.04 ± 0.27	0.96 ± 0.13	0.94 ± 0.12	N	Y
Q5F6P7	Putative amidase	amiC/NGO1502	1.56 ± 0.09	1.47 ± 0	1.32 ± 0.14	N	Y

Table II —*continued*

Accession	Name	Gene	Average ratio ± S.D.[a]			S[b]	T[c]
			F62:FA1090	MS11:FA1090	1291:FA1090		
Q5F932	Putative carboxy-terminal processing protease	NGO0572	0.82 ± 0.06	0.98 ± 0.36	0.84 ± 0.04	Y	N
Q5F759	Putative cytochrome	NGO1328	1.16 ± 0.01	1.2 ± 0.12	1.28 ± 0.23	N	Y
Q5FA09	Putative MafB-like protein	NGO0225	1.18 ± 0.17	1.2 ± 0.46	1.02 ± 0.01	Y	N
Q5F6X8	Putative Na(+)-translocating NADH-ubiquinone reductase subunit C	nqrC/NGO1415	1.1 ± 0.19	1.04 ± 0.16	1.11 ± 0.19	N	N
Q5F674	Putative outer membrane protein OmpU	ompU/NGO1688	1.73 ± 0.17	1.44 ± 0	1.54 ± 0.31	Y	N
Q5F8E6	Putative oxidoreductase	NGO0831	1.17 ± 0.1	1.33 ± 0.16	1.28 ± 0.25	N	N
Q5F766	Putative paraquat-inducible protein B	NGO1320	1.01 ± 0.02	0.98 ± 0.13	1 ± 0.01	N	N
Q5FAC8	Putative pilus assembly protein	pilM/NGO0098	1.11 ± 0.04	1.34 ± 0.17	1.48 ± 0.09	N	N
Q5F520	Putative uncharacterized protein	NGO2119	1.27 ± 0.05	1.03 ± 0.05	0.7 ± 0.18	Y	N
Q5F5E5	Putative uncharacterized protein	NGO1984	0.9 ± 0.04	0.98 ± 0.14	1.04 ± 0.04	N	N
Q5F5P4	Putative uncharacterized protein	NGO1873	1.34 ± 0.28	1.34 ± 0.1	0.94 ± 0.08	N	N
Q5F5W7	Putative uncharacterized protein	NGO1802	1.06 ± 0.18	1.45 ± 0.02	1.06 ± 0.19	Y	Y
Q5F657	Putative uncharacterized protein	NGO1709	1.22 ± 0.03	1.3 ± 0.07	1.44 ± 0.01	N	Y
Q5F676	Putative uncharacterized protein	NGO1686	1.11 ± 0.01	1.22 ± 0.03	1.29 ± 0	N	N
Q5F6K2	Putative uncharacterized protein	NGO1549	1.15 ± 0.09	1.1 ± 0.29	1.31 ± 0.03	N	Y
Q5F6P5	Putative uncharacterized protein	NGO1504	0.95 ± 0.08	1.38 ± 0.22	1.45 ± 0.09	N	N
Q5F7A6	Putative uncharacterized protein	NGO1274	1.41 ± 0.02	1.62 ± 0.1	1.46 ± 0.01	N	Y
Q5F7C7	Putative uncharacterized protein	NGO1251	0.94 ± 0.06	0.88 ± 0.39	0.62 ± 0.05	N	N
Q5FAK6	Putative uncharacterized protein	NGO0028	1.07 ± 0.17	1.44 ± 0.09	1.31 ± 0.36	N	N
Q5F9Q0	Signal peptidase I	lepB/NGO0343	1.01 ± 0.09	1.07 ± 0.12	1.21 ± 0.1	N	N
Q5F9E3	Type IV pilus assembly protein PilX	pilX/NGO0455	0.57 ± 0.06	0.74 ± 0.03	0.67 ± 0.12	N	N
O87406	UPF0070 protein NGO0425	NGO0425	1.11 ± 0.07	1.12 ± 0.22	0.98 ± 0.01	N	N

[a] Average ratios and standard deviations were calculated for proteins ubiquitously expressed in biological replica experiments.
[b] Predictions of signal peptide cleavage site using SignalP (47).
[c] Presence of twin-arginine signal peptide as determined by TatP (48).
[d] The surface localization of AniA was verified experimentally (97).
[e] The outer membrane localization of Ng-MIP was verified experimentally (78).

TABLE III
Ubiquitous proteins identified by iTRAQ in the GC MVs

Accession	Name	Gene	Average ratio ± S.D.[a]			S[b]	T[c]
			F62:FA1090	MS11:FA1090	1291:FA1090		
Outer membrane							
Q5F5F6	Adhesin mafA 1/4	mafA1/NGO1067 mafA4/NGO1972	0.97 ± 0.24	1.34 ± 0.36	1.25 ± 0.26	N	N
Q5F651	LPS-assembly protein lptD	lptD, imp, ostA/NGO1715	1.13 ± 0.25	1.5 ± 0.04	1.39 ± 0.27	Y	N
Q5F5V7	Major outer membrane protein porin P.IB	porB/NGO1812	1.35 ± 0.33	1.6 ± 0.26	1.1 ± 0.02	Y	N
Q5FAG7	Pilus-associated protein	pilC/NGO0055	1.38 ± 0.13	0.55 ± 0.03	0.97 ± 0.05	N	Y
Q5F6Q7	Phospholipase A1	pldA/NGO1492	0.97 ± 0.12	1.34 ± 0.22	1.29 ± 0.17	N	N
Q5F5W8	Putative uncharacterized protein	bamA/NGO1801	0.91 ± 0.07	1.21 ± 0.06	1.21 ± 0.04	Y	N
Q5FAD2	Type IV pilus biogenesis and competence protein pilQ	pilQ, omc/NGO0094	0.94 ± 0.1	1.34 ± 0.31	0.89 ± 0.15	Y	N
Periplasmic							
Q5F601	Catalase	katA/NGO1767	0.98 ± 0.45	0.93 ± 0.1	0.82 ± 0.25	N	N
Inner membrane							
Q5F823	Thiol:disulfide interchange protein DsbD	dsbD/NGO0978	1.24 ± 0.54	1 ± 0.34	1.44 ± 0.41	N	N
Unknown							
Q5F5U9	30S ribosomal protein S13	rpsM/NGO1821	0.97 ± 0.16	0.88 ± 0.13	0.91 ± 0.03	N	N
Q5F6H4	Adhesin mafA 2/3	mafA2/NGO1393;mafA3/NGO1584	1.22 ± 0.2	0.84 ± 0.04	0.92 ± 0.02	N	N
Q5F501	Lipoprotein	NGO2139	0.6 ± 0.09	0.81 ± 0.27	1 ± 0.05	Y	Y
Q5F9W2	IgA-specific metalloendopeptidase	iga/NGO0275	1.28 ± 0.16	1.35 ± 0.24	1.14 ± 0.37	Y	N
Q5F932	Putative carboxy-terminal processing protease	NGO0572	0.8 ± 0.1	1.54 ± 0.05	1.32 ± 0.4	Y	N
Q5FA09	Putative MafB-like protein	NGO0225	1.23 ± 0.37	0.94 ± 0.24	1.11 ± 0.05	Y	N
Q5FAC8	Putative pilus assembly protein	pilM/NGO0098	0.92 ± 0.13	0.76 ± 0.15	0.68 ± 0.17	N	N
Q5F576	Putative uncharacterized protein	NGO2054	0.97 ± 0.22	0.69 ± 0.07	1.48 ± 0.18	Y	N

[a] Average ratios and standard deviations were calculated for proteins ubiquitously expressed in both biological experiments.
[b] Predictions of signal peptide cleavage site using SignalP server (47).
[c] Presence of twin-arginine signal peptide as determined by TatP search engine (48).

brane, 5-periplasmic, 1-inner membrane, 32-cytoplasmic, and 10-unknown (Tables III and V, and supplemental Table S5).

In addition, the identified proteins were subjected to classification based on predicted major cellular function (Fig. 3). All phylogenetic Clusters of Orthologous Groups (COG) of proteins were represented within the cell envelopes (Fig. 3), with the majority of proteins predicted to be involved in cell motility and secretion (17%), cell envelope biogenesis (11%), and ribosomal function (17%). The latter COG was the most

TABLE IV
Differentially expressed GC cell envelope proteins identified by iTRAQ

Accession	Name	Gene	Average ratio ± S.D.[a]			S[b]	T[c]
			F62:FA1090	MS11:FA1090	1291:FA1090		
Outer membrane							
Q5F726	Multidrug efflux pump channel protein	mtrE/NGO1363	1.08 ± 0.04	2.65 ± 0.02	0.93 ± 0.15	Y	N
Q5F6Q4	Transferrin-binding protein A	tbpA/NGO1495	2.93 ± 0.25	0.83 ± 0.09	0.67 ± 0.07	Y	N
Periplasmic							
Q5F9E2	Putative type IV pilin-like protein	NGO0456	0.14 ± 0.04	1.11 ± 0.11	0.98 ± 0.05	N	N
Q5F724*	Antibiotic resistance efflux pump component MtrC[d]	mtrC/NGO1365	0.93 ± 0	2.98 ± 0.39	0.28 ± 0.06	Y	Y
Inner membrane							
Q5F725	Antibiotic resistance efflux pump component	mtrD/NGO1364	1.08 ± 0.01	3.21 ± 0.51	0.69 ± 0.02	N	N
Unknown							
Q5F5N1	Lipoprotein	NGO1889	2.56 ± 0.09	2.4 ± 0.45	3.35 ± 0.02	N	N
Q5F865	Putative peroxiredoxin family protein/glutaredoxin	NGO0926	0.39 ± 0.1	0.35 ± 0.11	0.27 ± 0.07	N	N
Q5F9E4	Type IV pilus assembly protein PilW	pilW/NGO0454	0.34 ± 0.09	0.24 ± 0.02	0.26 ± 0.06	N	N
Cytoplasmic							
Q5F5Q8	Elongation factor Tu	tuf1/NGO1842	0.41 ± 0.1	0.24 ± 0.03	0.3 ± 0.03	N	N
Q5F5T6	30S ribosomal protein S17	rpsQ/NGO1830	0.64 ± 0.23	0.41 ± 0.04	0.45 ± 0.02	N	N
Q5F5V3	50S ribosomal protein L17	rplQ/NGO1817	3.65 ± 0.07	1.7 ± 0.16	1.4 ± 0.05	N	Y

[a] Average ratio and standard deviation were calculated for differentially expressed proteins identified in both biological replica experiments with associated $p < 0.05$.
[b] Predictions of signal peptide cleavage site using SignalP server (47).
[c] Presence of twin-arginine signal peptide as determined by TatP (48).
[d] MtrC protein has been shown to be localized to the periplasm (111).

TABLE V
Differentially expressed proteins identified in naturally released MVs

Accession	Name	Gene	Average ratio ± S.D.[a]			S[b]	T[c]
			F62:FA1090	MS11:FA1090	1291:FA1090		
Outer membrane							
Q5F726	Multidrug efflux pump channel protein	mtrE/NGO1363	0.9 ± 0.07	2.73 ± 0.22	1.82 ± 0.15	Y	N
Q5F6Q4	Transferrin-binding protein A	tbpA/NGO1495	2.66 ± 0.42	1.2 ± 0.17	1.11 ± 0.22	Y	N
Periplasmic							
Q5FA17	ABC transporter, periplasmic binding protein, iron related	fbpA/NGO0217	2.58 ± 0.12	1.75 ± 0.03	4.8 ± 3.11	Y	N
Q5F6V7	Putative uncharacterized protein	dsbC/NGO1438	1.12 ± 0.04	2.38 ± 0.27	1.92 ± 0.56	Y	N
Q5F7W0	Putative uncharacterized protein	NGO1056	1.63 ± 0.18	1.41 ± 0.13	2.42 ± 0.32	N	Y
Q5F8C4	Putative uncharacterized protein	NGO0861	1.6 ± 0.46	2.2 ± 0.58	5.43 ± 3.25	Y	N
Unknown							
Q5F930	Carbonic anhydrase	cah/NGO0574	2.14 ± 0.33	2.27 ± 0.08	6.6 ± 4.16	Y	N
Q5F5H6	Putative uncharacterized protein	NGO1949	2.73 ± 0	1.22 ± 0.06	2.1 ± 0.31	Y	Y
Cytoplasmic							
Q5F905	Putative 30S ribosomal protein S1	rpsA/NGO0604	0.76 ± 0.15	0.5 ± 0	0.57 ± 0.17	N	N
Q5F5R4	50S ribosomal protein L7/L12	rplL/NGO1852	0.48 ± 0.01	0.31 ± 0.15	0.63 ± 0.03	N	N
Q5F9V6	Putative uncharacterized protein	NGO0282	1.06 ± 0.03	1.71 ± 0.08	2.33 ± 0.21	N	N

[a] Average ratio and standard deviation were calculated for differentially expressed proteins identified in both biological replica experiments with associated $p < 0.05$.
[b] Predictions of signal peptide cleavage site using SignalP (47).
[c] Presence of twin-arginine signal peptide as determined by TatP (48).

represented in the MVs fraction, followed by the functional category of proteins involved in cell envelope biogenesis (Fig. 3). COGs could not be assigned for 7 and 12% of proteins associated with the cell envelopes and MVs, respectively.

In conclusion, the subcellular distribution and biological functions of proteins identified in the GC cell envelope and MVs corroborated with previous studies assessing these proteome fractions in Gram-negative and Gram-positive bacteria (21, 63, 67, 69–76). Thus, our study adds to the growing amount of evidence that a large number of cytoplasmic proteins associates with cell envelope and MVs. Interestingly, similar observations come from proteomic profiling of membrane vesicles secreted from the plasma and endosomal membrane by various types of mammalian cells (77).

Ubiquitously Expressed Proteins Present in the GC Cell Envelopes and MVs—The quantitative analyses of relative protein abundance revealed that 305 and 46 proteins were uniformly present in the cell envelopes and MVs, respectively, in four GC strains (Tables II–III, supplemental Tables S4–S5). The large number of identified novel, and also previously described proteins precluded a detailed discussion, thus we focused only on several proteins assigned by bioinformatics

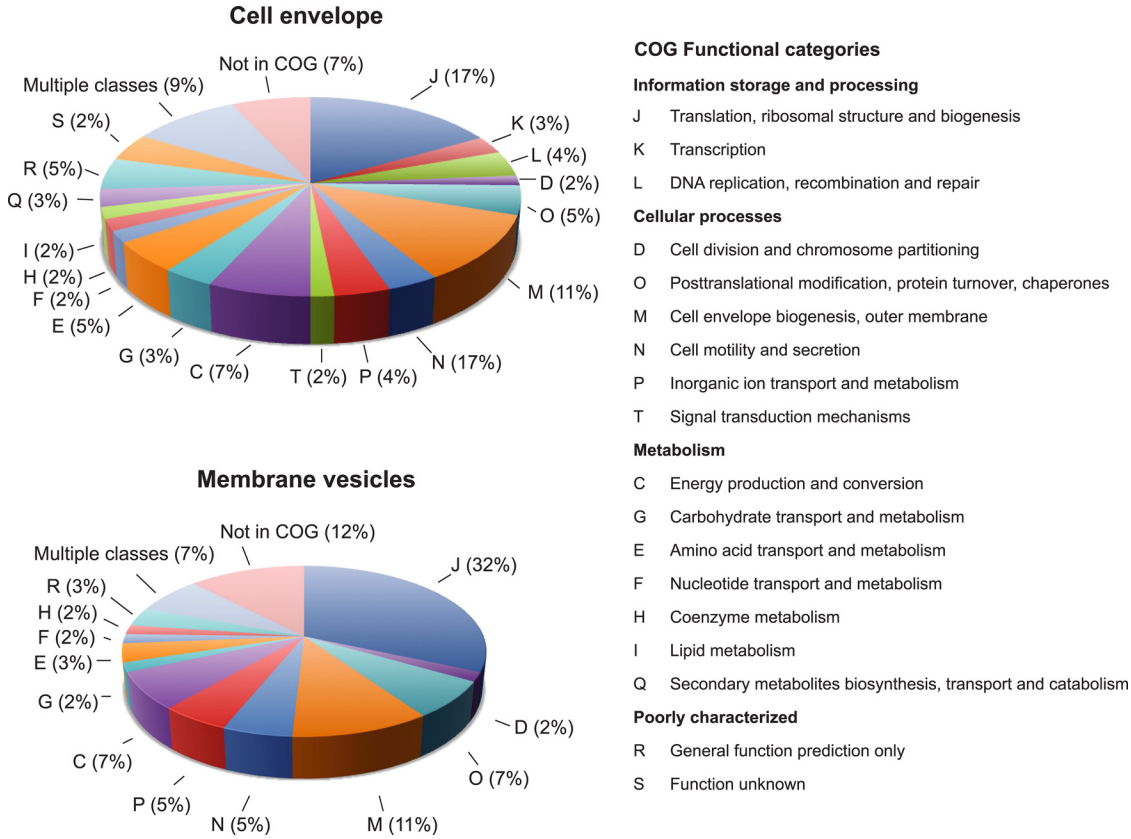

FIG. 3. **Functional classification of proteins identified in GC cell envelope and MVs according to clusters of orthologous groups (COGs).** The pie chart illustrates the percentages of identified proteins in each COG cluster. COG functional categories are listed on the right.

analyses either to the cell envelope or with unknown localization (Tables II–III).

Among the stably expressed cell envelope proteins, several previously uncharacterized in GC have been identified including LPS-transport protein LptD (formerly OstA, Imp), a protein designated in the SwissProt database as adhesion MafA 1/4, a putative TonB-dependent receptor, and eight predicted outer membrane proteins NGO1205, NGO0834, NGO2121, NGO2111, NGO1985, NGO1956, NGO1955, and NGO1344. A plethora of predicted periplasmic and inner membrane proteins as well as proteins with unknown localization were also discovered (Table II). Moreover, our experiments revealed ubiquitous expression of a number of recognized proteins including an outer membrane-localized enzyme, Phospholipase A, and a surface-exposed lipoprotein Ng-MIP (Table II). Concurring with our data, these proteins were found invariably expressed in many different GC and meningococcal isolates (78, 79). Perhaps not surprisingly, proteins participating in the process of outer membrane biogenesis, BamA (Omp85) and BamD (ComL), were identified by iTRAQ experiments as equally present in GC strains (Table II). The pivotal role of Bam proteins comprising the β-barrel assembly machinery have been recognized in both model organisms *E. coli* and *N. meningitidis*, reviewed in (80, 81). In GC, a peptidoglycan-linked lipoprotein, BamD, although not essential for cell viability, was required for efficient transformation by species-related DNA and its depletion- caused growth defects and altered colony morphology (82). Finally, OmpA-like protein and NGO1686 quantified in our proteomic studies (Table II), could serve as additional examples of ubiquitously expressed proteins that play crucial functions in the GC biology. OmpA, characterized by Serino *et al.*, is involved in the binding of GC to human cervical carcinoma and endometrial cells, entry into macrophages, intracellular survival in epithelial cells, and *in vivo* colonization (83). NGO1686 is a periplasmic, peptidoglycan-degrading peptidase and a virulence factor that protects GC against both nonoxidative polymorphonuclear leukocytes-mediated killing and oxidative-killing by hydrogen peroxide (84, 85). Together, these findings warrant further investigation of the newly discovered stably expressed proteins in the context of the GC general fitness and pathogenesis.

Our proteomic profiling of naturally shed MVs revealed a ubiquitous abundance of several outer membrane proteins including Phospholipase A, PorB, PilQ, adhesion MafA 1/4, and BamA (Table III). Sorting of these proteins into MVs was established in *N. meningitidis* and *N. lactamica* (75, 76, 78, 79, 86). One of the more fascinating features of a major GC porin, PorB (65) is its translocation from bacterial outer membrane and insertion into the membranes of eukaryotic cell organelles (87). It remains to be determined whether MVs play a role in

this process, however, experimental data from different pathogenic bacteria suggest that such a mechanism could be mediated via a direct adherence and internalization of MVs to host cells (16). Further, we discovered that LptD was also uniformly distributed into the MVs (Table III). Consistent with these results, sorting of LptD into the naturally released MVs was observed in other examined *Neisseriaceae*, *E. coli*, and *Pseudoaltermonas antarctica* (21, 75). The localization of this organic solvent tolerance protein into MVs might contribute to the bacterial survival under hostile conditions (21). Among other proteins present at similar levels in GC MVs were catalase, DsbD, and newly identified proteins including a predicted lipoprotein NGO2139, a putative carboxy-terminal processing protease NGO0572, and an uncharacterized protein NGO2054 (Table III). The intriguing location of catalase in MVs has also been reported in *Helicobacter pylori* (88). Further studies will be required to determine whether catalase is enclosed within the MVs or decorates their surface, perhaps because of the release of the cell contents after bacterial cell death. However, it is tempting to speculate that the MVs localization of this potent enzyme contributes to the remarkable resistance of GC against the oxygen-dependent mechanisms of bacterial killing within the human host. In addition, our experiments suggested that a virulence factor, which specifically cleaves human IgA1, extracellular metalloprotease IgA1 (89), was uniformly present in MVs isolated from GC strains (Table III). Although protease IgA1 was the first autotransporter described in *Neisseriaceae* (89), its presence in MVs has also been observed in *N. meningitidis* (86, 90, 91), which further suggests that IgA1 might be associated with the MVs.

Differentially Abundant Proteins in the GC Cell Envelopes and MVs—Considering the recognized differences between GC strains (Table I), it was not surprising that the iTRAQ experiments revealed 22 differentially abundant proteins in the cell envelopes and MVs (Fig. 2*E*, Tables IV–V). Worth noting, among the significantly altered proteins, were well-characterized components of the multidrug efflux-pump complex, MtrC-MtrD-MtrE, where "Mtr" corresponds to multiple transferable resistance. The orchestrated work of this three-component machinery provides an increased resistance to macrolide antibiotics, and antimicrobial compounds that GC might encounter in the human host including bile salts, progesterone, and antimicrobial peptide, LL37 (92–94). The relative abundance of the channel protein MtrE, the periplasmic accessory lipoprotein MtrC, and the inner membrane component MtrD was about threefold higher in the strain MS11 in comparison to that in FA1090 (Table IV). In contrast, strains F62 and 1291 displayed similar relative levels of Mtr constituents compared with FA1090. Consistently, the increased abundance of MtrE was observed in the MVs fraction isolated from strain MS11 (Table V). Warner *et al.* (94) revealed that the elevated expression of *mtr* operon in strain MS11 is because of a novel mutation, mtr_{120}, which yields the highest reported levels of Mtr-based resistance. In the same report, the authors provide experimental evidence for the correlation between an increased gradient of antimicrobial resistance and the levels of *in vivo* fitness. Indeed, studies in both the male urethritis model and in the murine model for GC infection clearly demonstrated that strain MS11 was more infectious than FA1090 (61). Interestingly, however, introducing the *mtr* mutation into strain F62 did not increase its infectivity (93), suggesting that another strain-dependent factor(s) might contribute to the levels of pathogenicity. Our iTRAQ experiments revealed previously unrecognized discrepancies between compared GC strains including differential abundance of NGO1889 encoding a putative lipoprotein, NGO0926 coding for a putative peroxiredoxin family protein, as well as putative uncharacterized proteins NGO1438, NGO1056, NGO0861, and NGO1949 (Tables IV–V). Future studies will establish whether these proteins represent virulence determinants contributing to the differential fitness observed between GC isolates.

Immunoblotting Analyses Confirm the iTRAQ Data—We were surprised that iTRAQ analyses indicated that AniA, which is an anaerobically induced surface-exposed outer membrane glycoprotein (95–97), was also ubiquitous in membrane fractions isolated from GC strains cultured aerobically (Table II). Therefore, we have chosen this protein as a first candidate for verification of our proteomic experiments. The gene encoding AniA (NGO1276) was cloned, overexpressed and a truncated soluble domain of AniA was purified to 95% purity as described under "Experimental Procedures." This purified antigen was used to immunize rabbits and obtain anti-AniA antibodies. Subsequently, the same amounts of cell envelope and MVs proteins (15 μg) extracted from GC strains FA1090, F62, MS11, and 1291 were separated by 4–20% gradient SDS-PAGE, transferred, and probed with anti-AniA antiserum. An example of such immunoblotting analysis is shown in Fig. 4*A*. As expected, there was a shift in migration of the purified truncated AniA (rAniA) in comparison to the native protein, which migrated at about 50 kDa. In agreement with the iTRAQ experiments, similar levels of AniA were present in the cell envelope fractions isolated from these four GC strains, and the protein was not detected in the MVs. Additionally tested GC strains including FA19 and a few clinical isolates (LG1, LG14, LG20, and LG26), expressed AniA at comparable levels during aerobic growth (Fig. 4*B*). As anticipated, the amounts of AniA were significantly decreased in comparison to that detected in bacteria cultured anaerobically in the presence of nitrite (Fig. 4*B*, FA1090 -O_2) (98).

To further validate iTRAQ experiments, the immunoblotting analyses of cell envelopes and MVs fractions isolated from FA1090, F62, MS11, and 1291 were performed with anti-Ng-MIP and anti-MtrE antisera (Fig. 4*A*). Overall, these studies confirmed iTRAQ quantifications. Similar levels of Ng-MIP were detected in all GC cell envelopes, whereas the level of MtrE was increased in strain MS11 (Table II and Fig. 4*A*). In addition, Ng-MIP was detected in the MVs fractions (Fig. 2*A*).

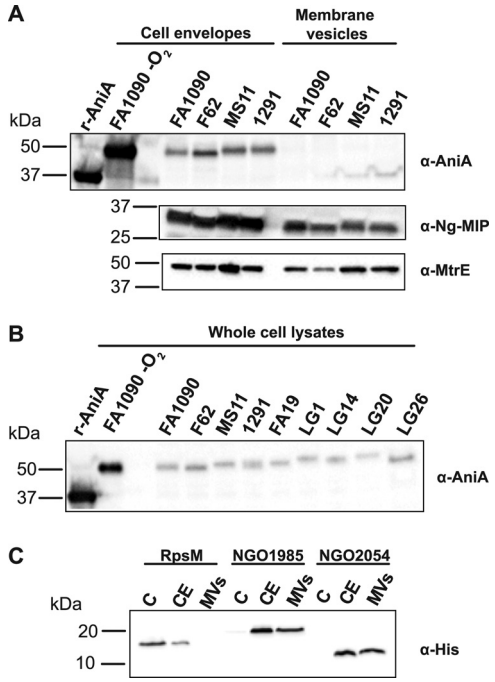

FIG. 4. **Immunoblotting analyses confirmed iTRAQ data.** *A*, Immunoblots, probed with either anti-AniA, anti-Ng-MIP, or anti-MtrE antiserum, of the cell envelopes and MVs extracted from different GC strains (as indicated above the panel). The total amounts of 15 μg of cell envelope and MVs proteins were loaded into individual wells and separated by SDS-PAGE on a 4–20% Tris-glycine gel. *B*, Whole-cell lysates derived from different GC isolates were resolved in a 4–20% Tris-glycine gel, transferred, and immunoblotting analysis was performed using rabbit antiserum against recombinant AniA. Samples containing whole-cell lysates were matched by equivalent OD_{600} units. Purified recombinant truncated version of AniA (250 ng, rAniA) and either cell envelope proteins (15 μg) or whole cell lysate from strain FA1090 grown anaerobically ($-O_2$) were used as positive controls. The designations of the strains are indicated at the top of the immunoblot. *C*, The subcellular distribution of RpsM, NGO1985, and NGO2054. Liquid cultures of GC FA1090 carrying either chromosomally expressed C-terminal-6×His-tagged RpsM, NGO1985, or NGO2054, were harvested, and subjected to the fractionation procedures. The total amounts of 15 μg of cytoplasmic (C), cell envelopes (CE), and MVs proteins were separated by SDS-PAGE on a 4–20% Tris-glycine gel, and probed with monoclonal anti-His antisera. The migration of molecular weight markers and their masses in kilodaltons (kDa) are indicated on the left.

This protein was identified by MS/MS but failed our rigorous criteria for protein quantification and thus was not included in the final list of 57 MVs proteins (Fig. 2*E* and supplemental Table S3).

Lastly, we aimed to evaluate the subcellular localization of several newly identified proteins. We have chosen predicted outer membrane protein NGO1985, and proteins with unknown localization NGO2139 and NGO2054. A homolog of ribosomal protein RpsM, NGO1821, and a periplasmic catalase, NGO1767, were also selected. We engineered an epitope-encoding tail, 6×His-tag, at the 3′ end of individual genes in their respective loci of FA1090 chromosome. Subsequently, liquid cultures of GC FA1090 carrying C-terminal-tagged proteins were harvested, subjected to the fractionation procedures, and processed for the detection of His epitope. The monoclonal anti-His antisera recognized recombinant RpsM, NGO1985, and NGO2054, which migrated according to their predicted molecular weight of 13.4-, 21.7-, and 10.5-kDa (Fig. 4*C*). The analysis failed to detect NGO1767 and NGO2139 (data not shown). Furthermore, these experiments showed that RpsM localized predominantly to the soluble fraction containing cytoplasmic proteins and was also present in the GC cell envelope, whereas both NGO1985 and NGO2054 were detected in the cell envelope and MVs fractions (Fig. 4*C*). Together, these results provided additional validation of our proteomic studies.

A Minor Outer Membrane Protein, LptD, is Essential in GC—The iTRAQ approaches led to the identification of 34 proteins that were ubiquitously expressed in four GC strains and identified in both cell envelopes and MVs fractions (Tables II–III). We propose that these proteins may represent attractive therapeutic targets, particularly if they are conserved throughout different GC strains and play an important biological function. As proof of principle, we focused on LptD, which was uniformly present in the cell envelopes and MVs in analyzed GC strains. This protein has not been previously characterized in GC, whereas in *E. coli*, LptD is an essential low-abundant outer membrane β-barrel protein involved in the cell envelope biogenesis (99). LptD is highly conserved among Gram-negative bacteria and plays a crucial function in transporting lipopolysaccharide into the outer leaflet of the outer membrane (100). Its role in the transport of lipopolysaccharide was first discovered in *N. meningitidis* but interestingly LptD was not found essential for the survival of this bacterium (101). To verify the notion that this gene is essential in GC (102), we engineered a strain in which chromosomal expression of *lptD* was placed under the control of IPTG-regulatable promoter, P_{lac}*lptD* (Fig. 5*A*). This strain grew robustly on GCB agar and in liquid media supplemented with 100 μM IPTG, whereas it was unable to form colonies upon direct plating from freezer stocks onto plates without IPTG (Fig. 5*B* and data not shown). Moreover, within three hours of culture in GCBL broth in the absence of IPTG there was a cessation of growth and at 5 hours the cell viability decreased almost 13-fold as compared with the strain expressing LptD (Fig. 5*B* and 5*C*). Consequently, upon depletion of LptD, the FA1090 P_{lac}*lptD* failed to form colonies when plated on solid media lacking IPTG (Fig. 5*D*). We noted, however, that sometimes a few colonies, likely carrying suppressor(s) mutations, were able to arise on this media (Fig. 5*C*). These colonies had drastically changed morphology as compared with that producing LptD. Individual colonies were characterized by an irregular edge; increase opacity, and a granular, rugose appearance (Fig. 5*D*). Growth defect and increase in colony opacity were also observed in *N. meningitidis lptD* mutant

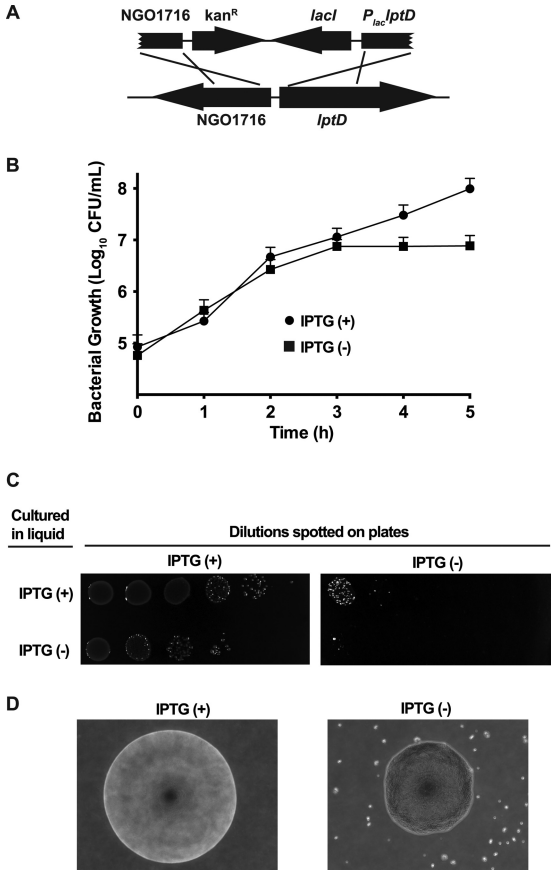

FIG. 5. **Effect of LptD depletion in GC.** *A*, Construction of an *lptD* conditional knockout in GC strain FA1090 was achieved by allelic replacement of the native *lptD* promoter with a DNA fragment containing IPTG-inducible promoter (P_{lac}), *lacI* gene, and a nonpolar antibiotic resistance cassette *apha3* (kan^R). *B,* FA1090 cells carrying chromosomal P_{lac}*lptD* were grown in the presence of 100 μM IPTG on GCB agar plates for 18 h. The bacteria were collected from plates, washed, divided, and growth was continued in the presence or absence of IPTG as indicated. Cell viability was monitored every hour by spotting serial dilutions onto GCB agar plates with (+) or without (-) IPTG, as indicated. Experiments were performed in biological quadruplicates and means and S.E. of colony forming units calculated per ml of bacterial cultures (CFU/ml) are presented. *C*, Representative experiments showing CFU's of strains spotted after 5 h onto GCB agar plates with or without IPTG. *D*, Representative micrographs illustrating the colony morphology of FA1090 P_{lac}*lptD* expressing LptD (+ IPTG) and upon depletion of LptD (− IPTG). GC colonies were visualized with a Zeiss AxioObserver.D1 microscope at A-Plan 10× magnification 0.25 Phase Contrast 1.

strain (101). Together, our observations support that LptD plays a pivotal function in GC.

A Lack of NGO1985 Dramatically Affects GC Cell Envelope Permeability Barrier—Finally, we have begun to address whether the newly identified proteins are important for GC physiology, and thus could serve as potential pharmacological targets. Six predicted outer membrane proteins with unknown function were selected for initial characterization including NGO1985, NGO1344, NGO1955, NGO2111, NGO2121, and NGO2139. These proteins were identified by iTRAQ as uniformly present in the cell envelopes derived from examined GC isolates (Table II). In addition, our fractionation experiments coupled with immunoblotting analyses showed that NGO1985 was localized to both cell envelope and MVs (Fig. 4*C*). The BLAST searches of the predicted amino acid sequences against NCBI and JCVI CMR (103) databases, revealed that all ORFs encode conserved hypothetical proteins with up to 50% identity throughout different species belonging to *Neisseriaceae*. Further, a presence of a putative membrane binding BON domain, **b**acterial **O**smY and **n**odulation, was identified in NGO1985. This domain is found in a family of osmotic shock protection proteins, a family of hemolysins, and a group of nodulation specificity proteins and secretory channels (104). The Omp85- and the AsmA-family domains, which are characteristics of proteins involved in the assembly of outer membrane, were identified in NGO1955 and NGO1344, respectively (105, 106).

The presence of these conserved domains suggested that these proteins function in the GC cell envelope homeostasis. To test this hypothesis, we first created in-frame deletions of individual genes. Subsequently the isogenic wild-type, FA1090, as well as Δ*ngo1985*, Δ*ngo1344,* Δ*ngo1955,* Δ*ngo2111,* Δ*ngo2121,* and Δ*ngo2139* were examined for their susceptibility toward a variety of compounds. All strains were suspended to 5×10^5 CFUs/ml, serially diluted, and plated on GCB agar either with or without different membrane-perturbing agents as well as chloramphenicol. An absence of individual proteins had no effect on GC growth under permissive conditions; however, loss of NGO1985 and NGO2121 resulted in significant inhibition of bacterial growth in the presence of bile salts and antimicrobial peptide, polymyxin B (Fig. 6*A*). Additionally, when compared with the parent strain, Δ*ngo1985* displayed dramatically decreased survival upon plating on media supplemented with detergents including Tween 20, SDS, and urea as well as chloramphenicol (Fig. 6*B*). This strong sensitivity phenotype was reversed in the complemented strain, Δ*ngo1985*/*Plac1985*, to the level observed in the wild-type bacteria (Fig. 6*A* and 6*B*). We concluded that loss of NGO1985, in particular, dramatically affected the general GC cell envelope permeability barrier. These studies further underscore the concept of ubiquitous cell envelope and MVs proteins as potential targets for new therapeutic interventions.

Final Remarks—Significant research in the GC field has been dedicated to elucidating the function and structure of several important virulence factors that are not stable because of both phase and antigenic variation. As such these proteins are not good candidates for developing therapeutic approaches. An example of this challenge was the monovalent pilus vaccine, which failed in a clinical trial (10). Our study began to establish a map of proteins in the cell envelope and MVs of a clinically relevant human pathogen. To the best of our knowledge, this is also the first time iTRAQ technology

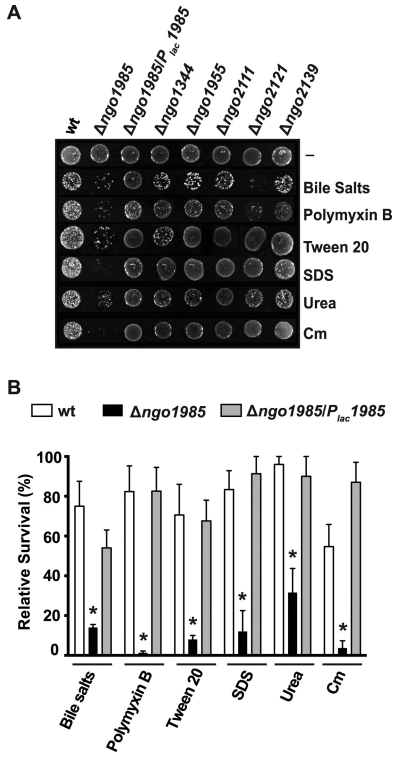

FIG. 6. **The GC cell envelope permeability barrier is compromised upon lack of NGO1985.** *A*, GC wild-type strain, FA1090 (wt), isogenic knockouts Δ*ngo1985*, Δ*ngo1344,* Δ*ngo1955,* Δ*ngo2111,* Δ*ngo2121,* Δ*ngo2139,* and complemented strain Δ*ngo1985/P*$_{lac}$*1985* were tested for sensitivity phenotypes to various compounds. All strains were suspended to 5×10^5 CFUs/ml, serially diluted, and plated on GCB agar either without (-) or with different compounds including bile salts (0.05%), polymyxin B (800 U), Tween 20 (0.005%), SDS (0.001%), urea (200 mM), chloramphenicol (0.2 μg/ml). Plates were inspected after 22 h of incubation in 5% CO_2 atmosphere at 37 °C. *B*, Experiments were performed as described above. The relative survival of parent strain, FA1090, Δ*ngo1985*, and complemented mutant, Δ*ngo1985/P*$_{lac}$*1985*, was calculated by comparing CFUs/ml on solid media containing the tested compound (as indicated) to the CFUs/ml on GCB agar. Experiments were performed on three separate occasions and the bars represent means with calculated S.E.. Statistically significant differences ($p < 0.05$) are indicated (*).

was used to elucidate the composition of bacterial MVs. Substantial research effort will be required to establish whether the proteins identified herein play important pathophysiological functions, to examine their phase and antigenic stability, and conservation throughout current GC clinical isolates, as well as their antigenic potency. Nevertheless, this study provides a framework for future research to elucidate the potential of the identified proteins as novel drug and vaccine targets.

Acknowledgments—We thank Dr. Josephine Bonventre for her excellent assistance, Dr. Stacey Harper (Department of Toxicology, OSU) for the use of the microscope, and Lisa Jones (Proteomics Facility, FHCRC) for assistance with performing proteomics experiments. We are grateful to Dr. Ann Jerse (Uniformed Services University, Bethesda, MD) for a generous gift of GC strains and anti-MtrE antisera. We thank Dr. Hank Seifert and Dr. Elizabeth Stohl (Northwestern University, Chicago, IL) for helpful discussion regarding GC complementation and plasmid pGGC4. We are thankful to Dr. Mariagrazia Pizza (Novartis Vaccines and Diagnostics, Siena, Italy) for providing the anti-Ng-MIP antisera. We also thank Dr. Robert Chalkley (University of California, San Francisco) and the PRIDE Team for their assistance in the mass spectrometry data deposition.

* This work was supported by the Medical Research Foundation of Oregon seed grant F0731A and the General Research Fund (OSU), as well as startup funds from OSU to AES. Additionally, we would like to acknowledge Undergraduate Research, Innovation, Scholarship and Creativity (OSU) for funding to J.V. Weber.

S This article contains supplemental Tables S1 to S5 and supplemental Material S1 to S4.

¶ To whom correspondence should be addressed: Department of Pharmaceutical Sciences, College of Pharmacy, Oregon State University, 419 Weniger Hall, 103 SW Memorial Pl., Corvallis, OR 97331. Tel.: 541.737.5811; E-mail: Aleksandra.Sikora@oregonstate.edu.

REFERENCES

1. Lusti-Narasimhan, M., and Ndowa, F. (2011) Emergence and spread of multi-drug resistant *Neisseria gonorrhoeae. J. Sex. Med.* **8,** 253
2. McNabb, S. J., Jajosky, R. A., Hall-Baker, P. A., Adams, D. A., Sharp, P., Worshams, C., Anderson, W. J., Javier, A. J., Jones, G. J., Nitschke, D. A., Rey, A., and Wodajo, M. S. (2008) Summary of notifiable diseases–United States, 2006. *MMWR Morb. Mortal. Wkly Rep.* **55,** 1–92
3. Edwards, J. L., and Apicella, M. A. (2004) The molecular mechanisms used by *Neisseria gonorrhoeae* to initiate infection differ between men and women. *Clin. Microbiol. Rev.* **17,** 965–981
4. Fleming, D. T., and Wasserheit, J. N. (1999) From epidemiological synergy to public health policy and practice: the contribution of other sexually transmitted diseases to sexual transmission of HIV infection. *Sex. Transm. Infect.* **75,** 3–17
5. Workowski, K. A., and Berman, S. (2010) Sexually transmitted diseases treatment guidelines, 2010. *MMWR Recomm. Rep.* **59,** 1–110
6. Yokoi, S., Deguchi, T., Ozawa, T., Yasuda, M., Ito, S., Kubota, Y., Tamaki, M., and Maeda, S. (2007) Threat to cefixime treatment for gonorrhea. *Emerg. Infect. Dis.* **13,** 1275–1277
7. Unemo, M., Shipitsyna, E., and Domeika, M. (2010) Recommended antimicrobial treatment of uncomplicated gonorrhoea in 2009 in 11 East European countries: implementation of a *Neisseria gonorrhoeae* antimicrobial susceptibility programme in this region is crucial. *Sex. Transm. Infect.* **86,** 442–444
8. Ison, C. A., Hussey, J., Sankar, K. N., Evans, J., and Alexander, S. (2011) Gonorrhoea treatment failures to cefixime and azithromycin in England, 2010. *Euro. Surveill.* **16**
9. Stoltey, J. E., and Barry, P. M. (2012) The use of cephalosporins for gonorrhea: an update on the rising problem of resistance. *Expert opin. Pharmaco.* **13,** 1411–1420
10. Zhu, W., Chen, C. J., Thomas, C. E., Anderson, J. E., Jerse, A. E., and Sparling, P. F. (2011) Vaccines for gonorrhea: can we rise to the challenge? *Front. Microbiol.* **2,** 124
11. Organization, W. H. (2012) Global action plan to control the spread and impact of antimicrobial resistance in *Neisseria gonorrhoeae.* p. 32, World Health Organization, Geneva
12. Prevention, C. f. D. C. a. (2013) Gonorrhea Treatment Guildlines. PMCID
13. Chan, Y. A., Hackett, K. T., and Dillard, J. P. (2012) The lytic transglycosylases of *Neisseria gonorrhoeae. Microb. Drug. Resist.* **18,** 271–279
14. Virji, M. (2009) Pathogenic *Neisseriae*: surface modulation, pathogenesis and infection control. *Nat. Rev. Microbiol.* **7,** 274–286
15. Cornelissen, C. N. (2008) Identification and characterization of gonococcal iron transport systems as potential vaccine antigens. *Future Microbiol.* **3,** 287–298
16. Ellis, T. N., and Kuehn, M. J. (2010) Virulence and immunomodulatory roles of bacterial outer membrane vesicles. *Microbiol. Mol. Biol. Rev.* **74,** 81–94

17. Pettit, R. K., and Judd, R. C. (1992) The interaction of naturally elaborated blebs from serum-susceptible and serum-resistant strains of *Neisseria gonorrhoeae* with normal human serum. *Mol. Microbiol.* **6,** 729–734
18. Pettit, R. K., and Judd, R. C. (1992) Characterization of naturally elaborated blebs from serum-susceptible and serum-resistant strains of *Neisseria gonorrhoeae. Mol. Microbiol.* **6,** 723–728
19. Kulp, A., and Kuehn, M. J. (2010) Biological functions and biogenesis of secreted bacterial outer membrane vesicles. *Annu. Rev. Microbiol.* **64,** 163–184
20. Britigan, B. E., Cohen, M. S., and Sparling, P. F. (1985) Gonococcal infection: a model of molecular pathogenesis. *N. Engl. J. Med.* **312,** 1683–1694
21. Lee, E. Y., Choi, D. S., Kim, K. P., and Gho, Y. S. (2008) Proteomics in gram-negative bacterial outer membrane vesicles. *Mass Spectrom. Rev.* **27,** 535–555
22. Greiner, L. L., Edwards, J. L., Shao, J., Rabinak, C., Entz, D., and Apicella, M. A. (2005) Biofilm Formation by *Neisseria gonorrhoeae. Infect. Immun.* **73,** 1964–1970
23. Steichen, C. T., Shao, J. Q., Ketterer, M. R., and Apicella, M. A. (2008) Gonococcal cervicitis: a role for biofilm in pathogenesis. *J. Infect. Dis.* **198,** 1856–1861
24. Falsetta, M. L., Steichen, C. T., McEwan, A. G., Cho, C., Ketterer, M., Shao, J., Hunt, J., Jennings, M. P., and Apicella, M. A. (2011) The composition and metabolic phenotype of *Neisseria gonorrhoeae* biofilms. *Front. Microbiol.* **2,** 75
25. Clark, V. L., Campbell, L. A., Palermo, D. A., Evans, T. M., and Klimpel, K. W. (1987) Induction and repression of outer membrane proteins by anaerobic growth of *Neisseria gonorrhoeae. Infect. Immun.* **55,** 1359–1364
26. Keevil, C. W., Davies, D. B., Spillane, B. J., and Mahenthiralingam, E. (1989) Influence of iron-limited and replete continuous culture on the physiology and virulence of *Neisseria gonorrhoeae. J. Gen. Microbiol.* **135,** 851–863
27. Yoo, J. S., Seong, W. K., Kim, T. S., Park, Y. K., Oh, H. B., and Yoo, C. K. (2007) Comparative proteome analysis of the outer membrane proteins of *in vitro*-induced multi-drug resistant *Neisseria gonorrhoeae. Microbiol. Immunol.* **51,** 1171–1177
28. Phillips, N. J., Steichen, C. T., Schilling, B., Post, D. M., Niles, R. K., Bair, T. B., Falsetta, M. L., Apicella, M. A., and Gibson, B. W. (2012) Proteomic analysis of *Neisseria gonorrhoeae* biofilms shows shift to anaerobic respiration and changes in nutrient transport and outermembrane proteins. *PLoS One* **7,** e38303
29. Brodeur, B. R., Johnson, W. M., Johnson, K. G., and Diena, B. B. (1977) *In vitro* interaction of *Neisseria gonorrhoeae* type 1 and type 4 with tissue culture cells. *Infect. Immun.* **15,** 560–567
30. Cohen, M. S., Cannon, J. G., Jerse, A. E., Charniga, L. M., Isbey, S. F., and Whicker, L. G. (1994) Human experimentation with *Neisseria gonorrhoeae*: rationale, methods, and implications for the biology of infection and vaccine development. *J. Infect. Dis.* **169,** 532–537
31. Kellogg, D. S., Jr., Cohen, I. R., Norins, L. C., Schroeter, A. L., and Reising, G. (1968) *Neisseria gonorrhoeae.* II. Colonial variation and pathogenicity during 35 months *in vitro. J. Bacteriol.* **96,** 596–605
32. Swanson, J. (1973) Studies on gonococcus infection. IV. Pili: their role in attachment of gonococci to tissue culture cells. *J. Exp. Med.* **137,** 571–589
33. Mickelsen, P. A., and Sparling, P. F. (1981) Ability of *Neisseria gonorrhoeae*, *Neisseria meningitidis*, and commensal *Neisseria* species to obtain iron from transferrin and iron compounds. *Infect. Immun.* **33,** 555–564
34. Kellogg, D. S., Jr., Peacock, W. L., Jr., Deacon, W. E., Brown, L., and Pirkle, D. I. (1963) *Neisseria gonorrhoeae.* I. Virulence Genetically Linked to Clonal Variation. *J. Bacteriol.* **85,** 1274–1279
35. Spence, J. M., Wright, L., and Clark, V. L. (2008) Laboratory maintenance of *Neisseria gonorrhoeae. Curr. Protoc. Microbiol.* Chapter **4,** Unit 4A 1
36. Morse, S. A., and Bartenstein, L. (1974) Factors affecting autolysis of *Neisseria gonorrhoeae*. *Proc. Soc. Exp. Biol. Med.* **145,** 1418–1421
37. Knapp, J. S., and Clark, V. L. (1984) Anaerobic growth of *Neisseria gonorrhoeae* coupled to nitrite reduction. *Infect. Immun.* **46,** 176–181
38. Cahoon, L. A., Stohl, E. A., and Seifert, H. S. (2011) The *Neisseria gonorrhoeae* photolyase orthologue phrB is required for proper DNA supercoiling but does not function in photo-reactivation. *Mol. Microbiol.* **79,** 729–742
39. Lai, E. M., Nair, U., Phadke, N. D., and Maddock, J. R. (2004) Proteomic screening and identification of differentially distributed membrane proteins in *Escherichia coli. Mol. Microbiol.* **52,** 1029–1044
40. Molloy, M. P., Herbert, B. R., Slade, M. B., Rabilloud, T., Nouwens, A. S., Williams, K. L., and Gooley, A. A. (2000) Proteomic analysis of the *Escherichia coli* outer membrane. *Eur. J. Biochem.* **267,** 2871–2881
41. Sikora, A. E., Zielke, R. A., Lawrence, D. A., Andrews, P. C., and Sandkvist, M. (2011) Proteomic analysis of the *Vibrio cholerae* type II secretome reveals new proteins, including three related serine proteases. *J. Biol. Chem.* **286,** 16555–16566
42. Saeed, A. I., Bhagabati, N. K., Braisted, J. C., Liang, W., Sharov, V., Howe, E. A., Li, J., Thiagarajan, M., White, J. A., and Quackenbush, J. (2006) TM4 microarray software suite. *Methods Enzymol.* **411,** 134–193
43. Gardy, J. L., Laird, M. R., Chen, F., Rey, S., Walsh, C. J., Ester, M., and Brinkman, F. S. (2005) PSORTb v. 2.0: expanded prediction of bacterial protein subcellular localization and insights gained from comparative proteome analysis. *Bioinformatics* **21,** 617–623
44. Imai, K., Asakawa, N., Tsuji, T., Akazawa, F., Ino, A., Sonoyama, M., and Mitaku, S. (2008) SOSUI-GramN: high performance prediction for subcellular localization of proteins in gram-negative bacteria. *Bioinformation* **2,** 417–421
45. Yu, C. S., Lin, C. J., and Hwang, J. K. (2004) Predicting subcellular localization of proteins for Gram-negative bacteria by support vector machines based on n-peptide compositions. *Protein Sci.* **13,** 1402–1406
46. Yu, C. S., Chen, Y. C., Lu, C. H., and Hwang, J. K. (2006) Prediction of protein subcellular localization. *Proteins* **64,** 643–651
47. Petersen, T. N., Brunak, S., von Heijne, G., and Nielsen, H. (2011) SignalP 4.0: discriminating signal peptides from transmembrane regions. *Nat. Methods* **8,** 785–786
48. Bendtsen, J. D., Nielsen, H., Widdick, D., Palmer, T., and Brunak, S. (2005) Prediction of twin-arginine signal peptides. *BMC Bioinformatics* **6,** 167
49. Tatusov, R. L., Koonin, E. V., and Lipman, D. J. (1997) A genomic perspective on protein families. *Science* **278,** 631–637
50. Wu, S., Zhu, Z., Fu, L., Niu, B., and Li, W. (2011) WebMGA: a customizable web server for fast metagenomic sequence analysis. *BMC Genomics* 12, 444 3180703
51. Horton, R. M., Hunt, H. D., Ho, S. N., Pullen, J. K., and Pease, L. R. (1989) Engineering hybrid genes without the use of restriction enzymes: gene splicing by overlap extension. *Gene* **77,** 61–68
52. Long, C. D., Tobiason, D. M., Lazio, M. P., Kline, K. A., and Seifert, H. S. (2003) Low-level pilin expression allows for substantial DNA transformation competence in *Neisseria gonorrhoeae. Infect. Immun.* **71,** 6279–6291
53. Skaar, E. P., Lazio, M. P., and Seifert, H. S. (2002) Roles of the *recJ* and *recN* genes in homologous recombination and DNA repair pathways of *Neisseria gonorrhoeae. J. Bacteriol.* **184,** 919–927
54. Menard, R., Sansonetti, P. J., and Parsot, C. (1993) Nonpolar mutagenesis of the ipa genes defines *IpaB*, *IpaC*, and *IpaD* as effectors of *Shigella flexneri* entry into epithelial cells. *J. Bacteriol.* **175,** 5899–5906
55. Dillard, J. P. (2011) Genetic manipulation of *Neisseria gonorrhoeae. Curr. Protoc. Microbiol.* Chapter **4,** Unit4A 2
56. Boulanger, M. J., and Murphy, M. E. (2002) Crystal structure of the soluble domain of the major anaerobically induced outer membrane protein (AniA) from pathogenic *Neisseria*: a new class of copper-containing nitrite reductases. *J. Mol. Biol.* **315,** 1111–1127
57. Dudas, K. C., and Apicella, M. A. (1988) Selection and immunochemical analysis of lipooligosaccharide mutants of *Neisseria gonorrhoeae. Infect. Immun.* **56,** 499–504
58. Schneider, H., Griffiss, J. M., Williams, G. D., and Pier, G. B. (1982) Immunological basis of serum resistance of *Neisseria gonorrhoeae. J. Gen. Microbiol.* **128,** 13–22
59. Swanson, J., Robbins, K., Barrera, O., Corwin, D., Boslego, J., Ciak, J., Blake, M., and Koomey, J. M. (1987) Gonococcal pilin variants in experimental gonorrhea. *J. Exp. Med.* **165,** 1344–1357
60. Cornelissen, C. N., Kelley, M., Hobbs, M. M., Anderson, J. E., Cannon, J. G., Cohen, M. S., and Sparling, P. F. (1998) The transferrin receptor expressed by gonococcal strain FA1090 is required for the experimental infection of human male volunteers. *Mol. Microbiol.* **27,** 611–616
61. Hobbs, M. M., Sparling, P. F., Cohen, M. S., Shafer, W. M., Deal, C. D.,

and Jerse, A. E. (2011) Experimental gonococcal infection in male volunteers: cumulative experience with *Neisseria gonorrhoeae* strains FA1090 and MS11*mkC. Front. Microbiol.* **2,** 123
62. *Neisseria gonorrhoeae* group Sequencing Project, Broad Institute of Harvard and MIT (http://www.broadinstitute.org/).
63. Papanastasiou, M., Orfanoudaki, G., Koukaki, M., Kountourakis, N., Sardis, M. F., Aivaliotis, M., Karamanou, S., and Economou, A. (2013) The *Escherichia coli* peripheral inner membrane proteome. *Mol. Cell. Proteomics.* **12,** 599–610
64. Dorward, D. W., Garon, C. F., and Judd, R. C. (1989) Export and intercellular transfer of DNA via membrane blebs of *Neisseria gonorrhoeae. J. Bacteriol.* **171,** 2499–2505
65. Johnston, K. H., and Gotschlich, E. C. (1974) Isolation and characterization of the outer membrane of *Neisseria gonorrhoeae. J. Bacteriol.* ***119,*** 250–257
66. Blake, M. S., and Gotschlich, E. C. (1982) Purification and partial characterization of the major outer membrane protein of *Neisseria gonorrhoeae. Infect. Immun.* **36,** 277–283
67. Poetsch, A., and Wolters, D. (2008) Bacterial membrane proteomics. *Proteomics* **8,** 4100–4122
68. Ross, P. L., Huang, Y. N., Marchese, J. N., Williamson, B., Parker, K., Hattan, S., Khainovski, N., Pillai, S., Dey, S., Daniels, S., Purkayastha, S., Juhasz, P., Martin, S., Bartlet-Jones, M., He, F., Jacobson, A., and Pappin, D. J. (2004) Multiplexed protein quantitation in *Saccharomyces cerevisiae* using amine-reactive isobaric tagging reagents. *Mol. Cell. Proteomics* **3,** 1154–1169
69. Tjalsma, H., Antelmann, H., Jongbloed, J. D., Braun, P. G., Darmon, E., Dorenbos, R., Dubois, J. Y., Westers, H., Zanen, G., Quax, W. J., Kuipers, O. P., Bron, S., Hecker, M., and van Dijl, J. M. (2004) Proteomics of protein secretion by *Bacillus subtilis*: separating the "secrets" of the secretome. *Microbiol. Mol. Biol. Rev.* **68,** 207–233
70. Dreisbach, A., van Dijl, J. M., and Buist, G. (2011) The cell surface proteome of *Staphylococcus aureus. Proteomics* **11,** 3154–3168
71. Lee, E. Y., Choi, D. Y., Kim, D. K., Kim, J. W., Park, J. O., Kim, S., Kim, S. H., Desiderio, D. M., Kim, Y. K., Kim, K. P., and Gho, Y. S. (2009) Gram-positive bacteria produce membrane vesicles: proteomics-based characterization of *Staphylococcus aureus*-derived membrane vesicles. *Proteomics* **9,** 5425–5436
72. Choi, D. S., Kim, D. K., Choi, S. J., Lee, J., Choi, J. P., Rho, S., Park, S. H., Kim, Y. K., Hwang, D., and Gho, Y. S. (2011) Proteomic analysis of outer membrane vesicles derived from *Pseudomonas aeruginosa. Proteomics* **11,** 3424–3429
73. Lee, E. Y., Bang, J. Y., Park, G. W., Choi, D. S., Kang, J. S., Kim, H. J., Park, K. S., Lee, J. O., Kim, Y. K., Kwon, K. H., Kim, K. P., and Gho, Y. S. (2007) Global proteomic profiling of native outer membrane vesicles derived from *Escherichia coli. Proteomics* **7,** 3143–3153
74. Berlanda Scorza, F., Doro, F., Rodriguez-Ortega, M. J., Stella, M., Liberatori, S., Taddei, A. R., Serino, L., Gomes Moriel, D., Nesta, B., Fontana, M. R., Spagnuolo, A., Pizza, M., Norais, N., and Grandi, G. (2008) Proteomics characterization of outer membrane vesicles from the extraintestinal pathogenic *Escherichia coli* Δ*tolR* IHE3034 mutant. *Mol. Cell. Proteomics* **7,** 473–485
75. Vaughan, T. E., Skipp, P. J., O'Connor, C. D., Hudson, M. J., Vipond, R., Elmore, M. J., and Gorringe, A. R. (2006) Proteomic analysis of *Neisseria lactamica* and *Neisseria meningitidis* outer membrane vesicle vaccine antigens. *Vaccine* **24,** 5277–5293
76. Gil, J., Betancourt, L. Z., Sardinas, G., Yero, D., Niebla, O., Delgado, M., Garcia, D., Pajon, R., Sanchez, A., Gonzalez, L. J., Padron, G., Campa, C., Sotolongo, F., Barbero, R., Guillen, G., Herrera, L., and Besada, V. (2009) Proteomic study via a non-gel based approach of meningococcal outer membrane vesicle vaccine obtained from strain CU385: a road map for discovering new antigens. *Hum. Vaccines* **5,** 347–356
77. Choi, D. S., Lee, J. M., Park, G. W., Lim, H. W., Bang, J. Y., Kim, Y. K., Kwon, K. H., Kwon, H. J., Kim, K. P., and Gho, Y. S. (2007) Proteomic analysis of microvesicles derived from human colorectal cancer cells. *J. Proteome Res.* **6,** 4646–4655
78. Leuzzi, R., Serino, L., Scarselli, M., Savino, S., Fontana, M. R., Monaci, E., Taddei, A., Fischer, G., Rappuoli, R., and Pizza, M. (2005) Ng-MIP, a surface-exposed lipoprotein of *Neisseria gonorrhoeae*, has a peptidyl-prolyl cis/trans isomerase (PPIase) activity and is involved in persistence in macrophages. *Mol. Microbiol.* **58,** 669–681
79. Bos, M. P., Tefsen, B., Voet, P., Weynants, V., van Putten, J. P., and Tommassen, J. (2005) Function of neisserial outer membrane phospholipase a in autolysis and assessment of its vaccine potential. *Infect. Immun.* **73,** 2222–2231
80. Hagan, C. L., Silhavy, T. J., and Kahne, D. (2011) β-barrel membrane protein assembly by the Bam complex. *Annu. Rev. Biochem.* **80,** 189–210
81. Bos, M. P., Robert, V., and Tommassen, J. (2007) Biogenesis of the gram-negative bacterial outer membrane. *Annu. Rev. Microbiol.* **61,** 191–214
82. Fussenegger, M., Facius, D., Meier, J., and Meyer, T. F. (1996) A novel peptidoglycan-linked lipoprotein (ComL) that functions in natural transformation competence of *Neisseria gonorrhoeae. Mol. Microbiol.* **19,** 1095–1105
83. Serino, L., Nesta, B., Leuzzi, R., Fontana, M. R., Monaci, E., Mocca, B. T., Cartocci, E., Masignani, V., Jerse, A. E., Rappuoli, R., and Pizza, M. (2007) Identification of a new OmpA-like protein in *Neisseria gonorrhoeae* involved in the binding to human epithelial cells and *in vivo* colonization. *Mol. Microbiol.* **64,** 1391–1403
84. Stohl, E. A., Chan, Y. A., Hackett, K. T., Kohler, P. L., Dillard, J. P., and Seifert, H. S. (2012) *Neisseria gonorrhoeae* virulence factor NG1686 is a bifunctional M23B family metallopeptidase that influences resistance to hydrogen peroxide and colony morphology. *J. Biol. Chem.* **287,** 11222–11233
85. Stohl, E. A., Dale, E. M., Criss, A. K., and Seifert, H. S. (2013) *Neisseria gonorrhoeae* metalloprotease NGO1686 is required for full piliation, and piliation is required for resistance to H2O2- and neutrophil-mediated killing. *MBio* **4**
86. Lappann, M., Otto, A., Becher, D., and Vogel, U. (2013) Comparative proteome analysis of spontaneous outer membrane vesicles and purified outer membranes of *Neisseria meningitidis. J. Bacteriol.* **195,** 4425–4435
87. Muller, A., Gunther, D., Brinkmann, V., Hurwitz, R., Meyer, T. F., and Rudel, T. (2000) Targeting of the pro-apoptotic VDAC-like porin (PorB) of *Neisseria gonorrhoeae* to mitochondria of infected cells. *EMBO J.* **19,** 5332–5343
88. Olofsson, A., Vallstrom, A., Petzold, K., Tegtmeyer, N., Schleucher, J., Carlsson, S., Haas, R., Backert, S., Wai, S. N., Grobner, G., and Arnqvist, A. (2010) Biochemical and functional characterization of *Helicobacter pylori* vesicles. *Mol. Microbiol.* **77,** 1539–1555
89. Pohlner, J., Halter, R., Beyreuther, K., and Meyer, T. F. (1987) Gene structure and extracellular secretion of *Neisseria gonorrhoeae* IgA protease. *Nature* **325,** 458–462
90. Post, D. M., Zhang, D., Eastvold, J. S., Teghanemt, A., Gibson, B. W., and Weiss, J. P. (2005) Biochemical and functional characterization of membrane blebs purified from *Neisseria meningitidis* serogroup B. *J. Biol. Chem.* **280,** 38383–38394
91. Ferrari, G., Garaguso, I., Adu-Bobie, J., Doro, F., Taddei, A. R., Biolchi, A., Brunelli, B., Giuliani, M. M., Pizza, M., Norais, N., and Grandi, G. (2006) Outer membrane vesicles from group B *Neisseria meningitidis* Δ*gna33* mutant: proteomic and immunological comparison with detergent-derived outer membrane vesicles. *Proteomics* **6,** 1856–1866
92. Jerse, A. E., Sharma, N. D., Simms, A. N., Crow, E. T., Snyder, L. A., and Shafer, W. M. (2003) A gonococcal efflux pump system enhances bacterial survival in a female mouse model of genital tract infection. *Infect. Immun.* **71,** 5576–5582
93. Warner, D. M., Folster, J. P., Shafer, W. M., and Jerse, A. E. (2007) Regulation of the MtrC-MtrD-MtrE efflux-pump system modulates the *in vivo* fitness of *Neisseria gonorrhoeae. J. Infect. Dis.* **196,** 1804–1812
94. Warner, D. M., Shafer, W. M., and Jerse, A. E. (2008) Clinically relevant mutations that cause derepression of the *Neisseria gonorrhoeae* MtrC-MtrD-MtrE Efflux pump system confer different levels of antimicrobial resistance and *in vivo* fitness. *Mol. Microbiol.* **70,** 462–478
95. Hoehn, G. T., and Clark, V. L. (1992) Isolation and nucleotide sequence of the gene (*aniA*) encoding the major anaerobically induced outer membrane protein of *Neisseria gonorrhoeae. Infect. Immun.* **60,** 4695–4703
96. Hoehn, G. T., and Clark, V. L. (1992) The major anaerobically induced outer membrane protein of *Neisseria gonorrhoeae*, Pan 1, is a lipoprotein. *Infect. Immun.* **60,** 4704–4708
97. Shewell, L. K., Ku, S. C., Schulz, B. L., Jen, F. E., Mubaiwa, T. D., Ketterer, M. R., Apicella, M. A., and Jennings, M. P. (2013) Recombinant trun-

cated AniA of pathogenic Neisseria elicits a non-native immune response and functional blocking antibodies. *Biochem. Biophys. Res. Commun.* **431,** 215–220
98. Householder, T. C., Belli, W. A., Lissenden, S., Cole, J. A., and Clark, V. L. (1999) cis- and trans-acting elements involved in regulation of *aniA*, the gene encoding the major anaerobically induced outer membrane protein in *Neisseria gonorrhoeae. J. Bacteriol.* **181,** 541–551
99. Braun, M., and Silhavy, T. J. (2002) Imp/OstA is required for cell envelope biogenesis in *Escherichia coli. Mol. Microbiol.* **45,** 1289–1302
100. Ruiz, N., Kahne, D., and Silhavy, T. J. (2009) Transport of lipopolysaccharide across the cell envelope: the long road of discovery. *Nat. Rev. Microbiol.* **7,** 677–683
101. Bos, M. P., Tefsen, B., Geurtsen, J., and Tommassen, J. (2004) Identification of an outer membrane protein required for the transport of lipopolysaccharide to the bacterial cell surface. *Proc. Natl. Acad. Sci. U.S.A.* **101,** 9417–9422
102. Tobiason, D. M., and Seifert, H. S. (2010) Genomic content of *Neisseria* species. *J. Bacteriol.* **192,** 2160–2168
103. Peterson, J. D., Umayam, L. A., Dickinson, T., Hickey, E. K., and White, O. (2001) The comprehensive microbial resource. *Nucleic Acids Res.* **29,** 123–125
104. Yeats, C., and Bateman, A. (2003) The BON domain: a putative membrane-binding domain. *Trends Biochem. Sci.* **28,** 352–355
105. Gentle, I. E., Burri, L., and Lithgow, T. (2005) Molecular architecture and function of the Omp85 family of proteins. *Mol. Microbiol.* **58,** 1216–1225
106. Deng, M., and Misra, R. (1996) Examination of AsmA and its effect on the assembly of *Escherichia coli* outer membrane proteins. *Mol. Microbiol.* **21,** 605–612
107. Cannon, J. G., Lee, T. J., Guymon, L. F., and Sparling, P. F. (1981) Genetics of serum resistance in *Neisseria gonorrhoeae*: the sac-1 genetic locus. *Infect. Immun.* **32,** 547–552
108. Carbonetti, N., Simnad, V., Elkins, C., and Sparling, P. F. (1990) Construction of isogenic gonococci with variable porin structure: effects on susceptibility to human serum and antibiotics. *Mol. Microbiol.* **4,** 1009–1018
109. Dillard, J. P., and Seifert, H. S. (2001) A variable genetic island specific for *Neisseria gonorrhoeae* is involved in providing DNA for natural transformation and is found more often in disseminated infection isolates. *Mol. Microbiol.* **41,** 263–277
110. Anderson, J. E., Hobbs, M. M., Biswas, G. D., and Sparling, P. F. (2003) Opposing selective forces for expression of the gonococcal lactoferrin receptor. *Mol. Microbiol.* **48,** 1325–1337
111. Hagman, K. E., Pan, W., Spratt, B. G., Balthazar, J. T., Judd, R. C., and Shafer, W. M. (1995) Resistance of *Neisseria gonorrhoeae* to antimicrobial hydrophobic agents is modulated by the *mtrRCDE* efflux system. *Microbiology* **141,** 611–622